AD-A054 460 CELANESE RESEARCH CO SUMMIT N J F/G 11/2
EFFECTS OF MOISTURE ON CHEMICAL INTERACTIONS AT A POLYMER-FIBER--ETC(U)
DEC 77 D E STUETZ, R E SULLIVAN, A DIEDWARDO F33615-76-C-5223
AFML-TR-77-214 NL

UNCLASSIFIED

1 OF 2
AD
A054460

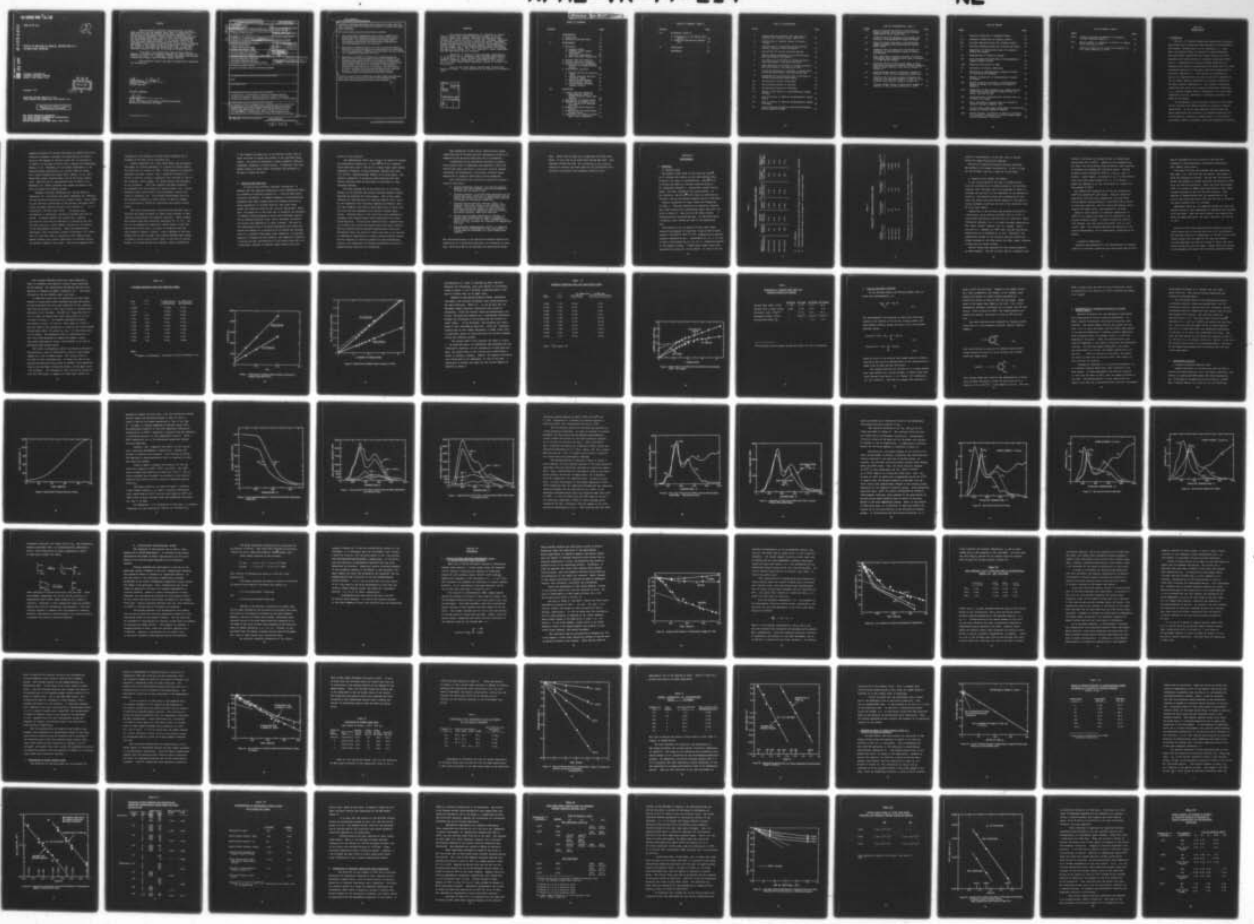

AFML-TR-77-214

2

EFFECTS OF MOISTURE ON CHEMICAL INTERACTIONS AT A POLYMER-FIBER INTERFACE

CELANESE CORPORATION
CELANESE RESEARCH COMPANY
SUMMIT, NEW JERSEY 07901

December 1977

TECHNICAL REPORT AFML-TR-77-214
FINAL REPORT FOR PERIOD MAY 1976-AUGUST 1977

AIR FORCE MATERIALS LABORATORY
AIR FORCE WRIGHT AERONAUTICAL LABORATORIES
AIR FORCE SYSTEMS COMMAND
WRIGHT-PATTERSON AIR FORCE BASE, OHIO 45433

NOTICE

When Government drawings, specifications, or other data are used for any purpose other than in connection with a definitely related Government procurement operation, the United States Government thereby incurs no responsibility nor any obligation whatsoever; and the fact that the government may have formulated, furnished, or in any way supplied the said drawings, specifications, or other data, is not to be regarded by implication or otherwise as in any manner licensing the holder or any other person or corporation, or conveying any rights or permission to manufacture, use, or sell any patented invention that may in any way be related thereto.

This report was submitted by the Celanese Research Company, a division of Celanese Corporation, under Contract No. F33615-76-C-5223. Dr. Lawrence T. Drzal, Mechanics and Surface Interactions Branch, was the AFML project monitor.

This technical report has been reviewed and is approved for publication.

Lawrence T. Drzal

Lawrence T. Drzal
Project Monitor

FOR THE DIRECTOR

S. W. Tsai

S. W. Tsai
Chief, Mechanics and Surface Interactions Branch
Nonmetallic Materials Division

SECURITY CLASSIFICATION OF THIS PAGE (When Data Entered)

REPORT DOCUMENTATION PAGE	READ INSTRUCTIONS BEFORE COMPLETING FORM
1. REPORT NUMBER: AFML-TR-77-214	2. GOVT ACCESSION NO. / 3. RECIPIENT'S CATALOG NUMBER
4. TITLE (and Subtitle): Effects of Moisture on Chemical Interactions at a Polymer-Fiber Interface.	5. TYPE OF REPORT & PERIOD COVERED: Technical Report. May 76 - Aug 77 / 6. PERFORMING ORG. REPORT NUMBER
7. AUTHOR(s): D.E. Stuetz, R.E. Sullivan, A. DiEdwardo, G. Hardy, O.D. Recca, [illegible] McMahon, J.R. Leal	8. CONTRACT OR GRANT NUMBER(s): F33615-76-C-5223
9. PERFORMING ORGANIZATION NAME AND ADDRESS: Celanese Corporation, Celanese Research Company, Summit, New Jersey 07901	10. PROGRAM ELEMENT, PROJECT, TASK AREA & WORK UNIT NUMBERS: 73403B3 / 03
11. CONTROLLING OFFICE NAME AND ADDRESS: Air Force Materials Laboratory, Air Force Systems Command, Wright-Patterson Air Force Base, Ohio 45433	12. REPORT DATE: Dec 77 / 13. NUMBER OF PAGES: 101
14. MONITORING AGENCY NAME & ADDRESS (if different from Controlling Office): Air Force Materials Laboratory, Nonmetallic Materials Division, Mechanics and Surface Interactions Branch	15. SECURITY CLASS. (of this report): Unclassified / 15a. DECLASSIFICATION/DOWNGRADING SCHEDULE

16. DISTRIBUTION STATEMENT (of this Report)

Approved for public release; distribution unlimited

17. DISTRIBUTION STATEMENT (of the abstract entered in Block 20, if different from Report)

Same

18. SUPPLEMENTARY NOTES

19. KEY WORDS (Continue on reverse side if necessary and identify by block number)

Graphite fibers, Graphite/Epoxy Composites, Humidity Exposure, Temperature Exposure, Moisture Absorption, Interface Properties, Mechanical Properties, Shear Strength Loss. Surface Area. Surface Groups.

20. ABSTRACT (Continue on reverse side if necessary and identify by block number)

The objective of this investigation was to determine the effects of moisture and temperature on chemical interactions at the interface of a specific graphite fiber/epoxy resin composite. Studies to evaluate these effects comprised the determination of the number and type of surface sites on a Celion® GY-70 graphite fiber, that react with epoxy groups; the measurement of the rate of degradation of these sites under dry and humid

over

DD FORM 1 JAN 73 1473 EDITION OF 1 NOV 65 IS OBSOLETE

UNCLASSIFIED

SECURITY CLASSIFICATION OF THIS PAGE (When Data Entered)

401 863

conditions at elevated temperatures; and a comparison of these rates with rates of the irreversible loss of interface properties of graphite fiber/epoxy resin composites.

The results of the work may be summarized as follows:

1. The concentration of epoxidizable surface sites on Celion^{R} GY-70 graphite fiber was 1.85μM/gm covering 1.5% of the total available fiber surface. The surface sites showed a 96/4 molar ratio of carboxyl/hydroxyl groups and commenced thermal degradation at 320°C with formation of CO, CO_2, and water.

2. Degradation of epoxidized surface sites under dry and wet conditions followed a first order rate with an activation energy of 16.3 Kcal/mole. The rate of degradation at 100% R_H was ten fold that of the rate at 0% R_H, over a temperature range of 100°C to 210°C.

3. Degradation of Celion^{R} GY-70/epoxy resin composites (Epi-Rez 508/p, p'-diamino diphenylsulfone) under the same conditions as for epoxidized surface sites caused an irreversible loss of interlaminar shear strength (ILSS) whose rate decreased with time of exposure and tended towards a constant level. The initial rate of ILSS decay showed an activation energy of 6.6 Kcal/mole. This was the same as that for the initial rate of moisture absorption into the composite specimen. Flexural strength and flexural modulus were not irreversibly affected by the thermal or hydrolytic treatment.

From these results it was concluded that cleavage of fiber/resin interface bonds may be discounted as the source for the irreversible strength losses experienced in graphite fiber/epoxy resin composites.

FOREWORD

This report was prepared by Dr. Dagobert E. Stuetz, Research Associate, Celanese Research Company, 86 Morris Avenue, Summit, New Jersey. The work was performed under Contract No. F33615-76-C-5223, Project No. 734003B3, sponsored by the Mechanics and Surface Interactions Branch (AFML/MBM), Nonmetallic Materials Division of the Air Force Materials Laboratory (AFML), Air Force Systems Command, Wright-Patterson Air Force Base, Ohio. The time period covered by the effort was May 1976 to August 1977. Dr. Lawrence T. Drzal (AFML/MBM) was the laboratory project engineer.

Besides D. E. Stuetz as the principal investigator, R. E. Sullivan and A. DiEdwardo (ESCA and Mass Spectrometry), G. Hardy and O. D. Recca (Surface Area Measurements), and P. McMahon (Composite Preparation) contributed to this effort. Dr. J. R. Leal, Senior Staff Associate, served as contract administrator.

This is the Final Report issued under Contract No. F33615-76-C-5223. It was submitted by the authors on November 1, 1977.

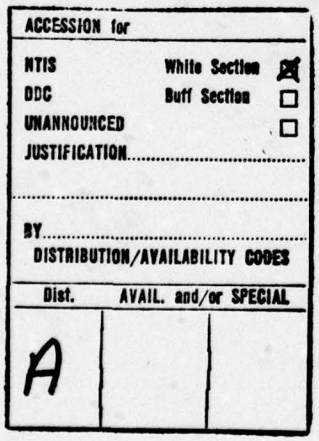

TABLE OF CONTENTS

TABLE OF CONTENTS (CONT'D)

LIST OF ILLUSTRATIONS

LIST OF ILLUSTRATIONS (CONT'D)

LIST OF TABLES

LIST OF TABLES (CONT'D)

SECTION I
INTRODUCTION

1. HISTORICAL

The loss of elevated temperature properties of graphite fiber/epoxy resin composites after exposure to high humidity environments became known in 1970 (Reference 1). Since then, the adverse effect of moisture on these composites has been broadly classified into losses related to matrix properties and those related to interface properties (Reference 2). Deterioration of matrix related properties is primarily the result of plasticization by water and of a sharp concurrent reduction of the glass transition temperature of the resin (Reference 3). This process is reversible by drying the composite below its glass transition temperature, and an almost complete restoration of original properties has been reported (Reference 4). By contrast, interfacial properties were shown to be largely irreversible (Reference 5, 6), whereby thermal spiking (Reference 7) or even modest temperature cycling (Reference 8) increases the extent and speed of the damage.

The mechanism by which moisture interacts at the fiber/matrix interface and affects mechanical properties remains unexplained. It is not clear whether covalent bonds are being ruptured at the interface, by stresses resulting from plasticization, relaxation, thermal motion, or by reaction with water; whether dispersion forces are weakened by moisture;

or ionic bonds are dissociated; whether water accumulates at the interface and reduces physical bonding; or whether a combination of these factors controls the effects observed. Kaelble, et al. have proposed an ionic mechanism for interfacial degradation (Reference 5, 9). In essence, he suggests that surfaces with a high dispersion (γ_d) and low ionic (γ_i) contribution to the surface energy (γ) and, in addition, with $\gamma^2 = \gamma_d^2 + \gamma_i^2 \geq 36$ dynes/cm^2 to insure wetting, are necessary for the production of interfaces which are moisture insentitive. Using these concepts and invoking the Griffith criterion for failure, he generated (theoretical) data which agree well with experimental results on the moisture sensitivity of composite materials.

A similar uncertainty exists concerning the type and concentrations of surface groups on graphite fibers which are capable of forming covalent bonds with epoxy resin. The major effort in the area of surface group analysis has traditionally been concentrated on graphite and active carbons, e.g., carbon blacks. Only recently, the study of carbon and graphite fiber surfaces has begun. However, data accumulation is rendered difficult because of the smaller surface areas of fibers, as compared to the high specific surface area of carbon blacks, resulting in a drastic reduction in the bulk concentration of surface species. Although it is generally accepted that the surfaces of active carbons and carbon fibers, are populated by several oxygen containing

species --- carboxyl, phenol, lactone, and quinoid-type groups --- their presence may or may not be important for the interface bonding behavior. Thus, Herrick, et al. (Reference 10) have determined surface group concentrations on nitric acid treated carbon and graphite fibers, using a titration method. They found that interlaminar shear strength (ILSS) increased with increasing surface groups (mostly of the phenolic and carboxyl type). Scola, et al. (Reference 11) and Ergun (Reference 12), on the other hand, could not confirm such a correlation.

A variety of other techniques have been developed for the analysis of surface properties: spectroscopic, thermal decomposition, gaseous and liquid adsorption, gas chromatography, and wetting behavior. Most of these methods cannot provide reliable quantitative data regarding the concentrations of surface groups.

The wetting behavior of carbon fibers has been determined by Chwastiak (Reference 13) and Herrick (Reference 10) who measured contact angles and found that water was the liquid most sensitive to changes of surface properties of yarns. Oxidation treatment was found to lead to improved wetting. Scola and Brooks described two techniques for characterizing the surfaces of carbon fibers. In a gas chromatographic method (Reference 14) the pulse retention times (prt) were measured for various vapors --- the sample fibers being used as the column. Prt was seen to reflect changes in surface properties. Adsorption of ionic solutions (Reference 15) was used to

measure the effect of various treatments on surface reactivity. Oxidative treatment increased the concentration of anionic sites at the expense of cationic sites, but no correlation to ILSS or to the type of resin-fiber bonding was established. Walker, et al. (Reference 16) and others (Reference 17, 18) measured oxygen chemisorption on various forms of carbon. For a highly graphitized carbon black, Walker, et al. estimated that oxygen occupied about 2.6% of the total surface area. Based on the IR spectroscopy work of Smith, et al. (Reference 19), Walker proposed that oxygen was bound in the form of lactone and carbonyl groups.

Mimeault and McKee (Reference 20), Moller and Fort (Reference 21), and Perkins and Smith (Reference 22), measured the gas evolution during heat-up of carbon fibers. Below 500°C, CO_2 was the major consitutent of the off-gas; and above 500°C, CO was the major species evolved, with H making a significant contribution (20-25%) above 800°C. Concurrent with off-gassing, a significant increase of surface area was observed. As Walker himself has pointed out, however, the value of this type of experiment is limited by the fact that gas evolution curves depend critically on the details of the experimental conditions. Among the spectroscopic techniques, total attenuated internal reflectance I.R. (Reference 23), has been used in conjunction with carbon blacks. Ketone carbonyl was clearly identified, but neither quinone nor phenolic hydroxyl were found. Perkins has employed this

technique for the analysis of carbon fiber surfaces, but a synopsis of her work is not available yet.

Koenig (Reference 24), using laser Raman, has determined the amount of "crystal boundary" in a series of carbon fibers and found that it relates to ILSS. X-ray analysis of fractured specimens revealed, however, that a graphitic structure remained in pullout cavities, suggesting that the mode of failure was "probably" shear within the fibers rather than debonding at the interface. This idea supports the model presented by Diefendorf for the structure of carbon fibers, i.e., circumferential cracks which result from anisotropic thermal contraction (Reference 25). Since Raman spectroscopy relies on the analysis of homolytic carbon bonds, it does not appear to be particularly suited for characterizing surface treated fibers.

The final spectroscopic technique which has been used to evaluate the bonding schemes on carbon fiber surfaces is ESCA (electron spectroscopy for chemical analysis). Three independent studies have been conducted (Reference 26, 27, 28). Donnet, et al. compared the spectra of carbon fibers, virgin and treated with nitric acid, to those of graphite oxide and some aromatic (organic) liquids. From a shoulder on the high energy side of the C_{1s} peak, the authors concluded that oxygen is bound in nitric acid treated fibers in the form of ketones. Barber, et al. have pointed out, however, from an examination

of the breadth and magnitude of the chemical shifts, that at least two kinds of oxygen are present in all oxidized carbon fibers. One cannot be assigned to simple aliphatic carbonyls, aldehydes, carboxyls, or amide groups. In addition, the total oxygen content of these fibers (oxidized) was estimated to be about 5 atomic per cent.

2. OBJECTIVE AND WORK PLAN

In view of the currently available information, it appears that the operative mechanism(s) which determines ILSS--- as a measure of interface properties --- has not been satisfactorily elucidated. If adhesive bonding is the determining parameter,then fiber surface area and roughness would be of prime importance; if covalent bonding, then their total number and stability would be the critical determinant. Therefore, the objective of this work was to establish the existence of chemical bonding between an epoxy resin polymeric species and an uncoated graphite fiber, and to determine the effect of moisture and temperature on these linkages. The goal of the investigation was to provide experimental data which permitted the drawing of a conclusion as to whether the strength loss of a graphite fiber/epoxy resin composite, on long-term expsoure to temperature and humidity, was chemical or physical in nature and what contributions to this effect were due to an irreversible cleavage of chemical bonds between fiber and

matrix at the interface.

The experimental effort was limited, by reason of economy and experimental simplicity, to Celion® GY-70 as a graphite fiber substrate, and to the use of a simple epoxy resin system composed of bisphenol A diglycidylether (Epi-Rez 508) with p,p'-diamino diphenylsulfone (DADPS) as a curing agent. The implicit assumption in selecting these materials was that results obtained would be applicable in principle to other analogous systems.

The work planned was to be carried out on two master batches of non-oxidized and surface oxidized graphite fibers, acquired and reserved for this prupose. The initial phase involved the identification of reactive surface sites, going on the assumption that they were composed of carboxyl, phenolic OH, carbonyl, and lactone functionalities, of which only the first two were expected to be reactive towards epoxy groups. Differentiation of the sites was to be attempted by treatment with reagents which react selectively with these functionalities. To facilitate identification, reagents were to be chosen that contained halogen which was easily identifable by induced electron emission spectroscopy. Additional information about the nature of these sites was to be obtained by degradation experiments of surface reacted graphite fibers and the analysis of volatile products by mass spectroscopy. Likewise, the hydrolytic and thermal degradation kinetics of tagged surface sites was to be measured.

Upon completion of the initial identification phase, composites were to be made and their degradation kinetics at temperature and moisture conditions was to be measured.

A comparison of the degradation behavior of surface sites against that of composites was expected to yield the desired data base from which a conclusion could be reached concerning the mechanism of irreversible strength losses experienced in graphite fiber/epoxy resins composites.

The investigation was carried out along five parallel lines of activities.

a. Surface Reactions (Tagging): to provide starting material with identifiable sites for instrumental analysis and the kinetic work.

b. Reaction Kinetics: to provide data pertaining to the thermo/hydrolytic stability of epoxidizable surface groups for correlation with analogous data obtained from graphite fiber/epoxy composites.

c. *Induced Electron Emission* Analysis (ESCA): to identify functional groups on the graphite fiber surface. Since ESCA yields only the number of functional groups per number of carbons counted on a relative scale, supporting data from neutron activation analysis (NAA) were obtained.

d. Vacuum Pyrolysis/Mass Spectrometry (VPy/MS): to provide data concerning the type of oxygenated surface species in terms of their degradation products (CO, CO_2, and H_2O) as a function of temperature and time.

e. Pyrolysis/Gas Chromatography (Py/GC): to quantify VPy/MS data by measurement of the total amount of a given species liberated at a given temperature interval.

The interrelationship of the analytical methods required the acquisition of a broad data base prior to correlation of data. Thus, Py/GC data had to be available for quantifying VPy/MS

data. These could be used for a comparison with ESCA data which, in turn, had to be quantified through NAA data. Both together yielded the base for evaluation of the reaction kinetics to extract pertinent data for the correlation with strength loss results from composite stability work.

SECTION II

EXPERIMENTAL

1. MATERIALS

a. Graphite Fiber

The graphite fiber used in this work was Celion® GY-70, because the surface of this high modulus fiber contains a low level of contamination. Celion® GY-70 is usually provided as a surface oxidized material. For comparison purposes, a non-surface treated control sample has been included in the investigation. In the following, the Celion® GY-70 fiber is identified as ST-fiber, and the non-surface treated control as GR-fiber.

Physical properties of these fibers are summarized in Table I. Physical properties of composites prepared from these fibers with a proprietory epoxy type resin are given in Table II. Data are for 69% fiber loading a unidirectionally oriented specimen. As described below, a different resin system was used in the degradation work.

The analysis of 10 gm samples of both fiber types revealed the presence of less than 75 ppm of ash as metal oxides. A qualitative assay of this composition by emission analysis indicated as major constituents Si, Fe, V, Ti, and as minor constituents Mg, Al, Ca, Cu, in descending amounts in the sequence listed. A quantitative assay would have required the ashing of a 100 gm sample. In view of the low

TABLE I

PHYSICAL PROPERTIES OF GRAPHITE FIBERS

Package (a) Identification	Surface Treated	Average Denier Per Fil	Density (b) (g/cc)	Average Cross-Section (10^{-8} in^2)	Tensile(c) Strength (10^3 psi)	Tensile(c) Modulus (10^6 psi)
GR/3-152/01	No	0.96	1.948	8.48	319	70.0
GR/3-152/02	No	0.96	1.963	8.41	319	70.0
ST/3-152/03	Yes	0.96	1.965	8.40	250	72.6
ST/3-152/04	Yes	0.96	1.964	8.41	250	72.6

a) 4 lb. packages

b) Density determined by the sink-float method in ethylene dibromide/toluene solutions.

c) Tensile properties based on an average of 20 single filament breaks.

TABLE II

COMPOSITE[a] PROPERTIES OF GRAPHITE FIBERS

Package Indentification	Flex Strength (10^3 psi)	Flex Modulus (10^6 psi)	Interlaminar Shear[b] Strength (psi)
ST/3-152/03	121	43.2	10,600
ST/3-152/04	141	42.2	10,800
GR/3-152/01	95	43.2	2,800
GR/3-152/02	95	43.2	2,800

[a] Epoxy-Novolac resin matrix material, 69% fiber loading, unidirectional specimen

[b] Determined by Short Beam Bending with a 4/1 Span-to-Depth ratio

levels of contamination, it was felt that no further effort for quantification was required.

Results of a neutron artivation analysis indicated the presence of an oxygen concentration of 352 ± 43 ppm for the ST-fiber, and 56 ± 5 ppm for the GR-fiber.

b. Graphite Fiber Powder (ST-Powder)

In the initial phase of the work it became obvious that the concentration of surface groups on the available graphite fiber (ST-type) had to be increased in order to increase the precision of the assessment of the degradation kinetics. The approach chosen was to powderize GR type fiber and expose the high surface samples to the same oxidizing treatment conditions as used in the conversion from GR to ST type fibers.

Comminution of the GR fiber was achieved by grinding in a Wiley mill, or by cutting the fiber into ca. 0.125 in. long pieces followed by cryo-milling in a mixer/mill (SPEX Industries, Metuchen, N.J.) at liquid nitrogen temperatures. The Wiley milled samples had an average particle size of 7μ diameter by 1000μ long, and the cryo-milled samples were 3μ in diameter by 3μ long. Obviously, the comminution process in the cryo-mill was more severe and caused cleavage of the fiber along the fiber length, exposing a large area of virgin surface.

Several routes were explored for the surface oxidation of these powders. One was to carry them on a graphite tape

through a continuous air oxidation oven at temperatures ranging from 450 to 850°C. Composites were prepared from the tapes, and interlaminar shear strengths (ILSS) measured, to determine the appropriate treatment regime. Optimum properties were obtained at 825°C at 11300 psi ILSS. In another, a small sample was heated in air in a TGA furnace until the weight loss reached 5 wt. %. In a third, a sample was exposed to air for ten minutes in a muffle furnace heated to 850°C.

All samples were analyzed for CO and CO_2 evolution at 1000°C by pyrolysis/GC (see below). They all showed the same 65/35 ratio of CO/CO_2 composition, with the Wiley milled samples indicating about a three-fold higher amount of total gas evolution, and the cryo-milled samples about a twelve fold higher level, than observed on ST-fiber.

Based on these results, an oxidation temperature of 850°C for 10 minutes was chosen as the standard for the surface oxidation regime. A muffle furnace was used for this purpose, with the cryo-milled powder held in a porcelain dish. The resulting material was employed in the kinetic measurements, and is subsequently identified as ST-powder.

c. Composite Preparation

Composite specimens used for the determinations of thermal effects on interface properties were fabricated from ST-fiber

tape by impregnation with a mixture of Epi-Rez 508 (bisphenol A diglycidylether) and diamino diphenylsulfone (DADPS) curing agent.

A new batch of resin was prepared each day composites were made, i.e., the resin was not stored. Each batch of resin was prepared as follows. Epi-Rez 508 (100 parts by weight) was placed in a metal container and heated to 130°C in an oil bath with stirring. After the resin had reached 130°C, 35.4 parts of DADPS (100% stoichiometry) were added in small portions to the hot 508 with stirring. Slow addition of DADPS assured that the temperature of the mixture was maintained above 120°C and the time to dissolve the amine hardener kept to a minimum.

Immediately after all the DADPS had melted, the resin was rapidly cooled to room temperature by immersing the container into cold water. When the resin mixture was properly prepared (as described above) the resin viscosity was 900 cps at 70°C.

Strips of GY-70 tape containing 300 parallel yarns were tautly taped onto a rotating drum with a 30" circumference. The drum was heated to a temperature of 70-80°C and the resin slowly poured onto the tapes as the drum was rotated. A tongue depressor was used as a blade to doctor the resin evenly across and into the tapes. Excess resin was removed by overwrapping the tapes with non-woven polyester bleeder

paper and hand rolling with a wider rubber roll to squeeze excess resin into the bleeder.

The prepreg, containing 60% (by weight) of resin, was transferred onto a flat surface and folded from a 3" width down to 0.25" wide by 12" long strips. Six of these strips were placed into a steel matched die mold.

For curing, the mold was transferred into a press, contact pressure (5 PSI) applied, and heated to 150°C. After 20 minutes, the pressure was raised to 100 PSI, held there for 40 minutes, then the temperature raised to 177°C, held for 90 minutes, and finally heated to 204°C, and held for 90 minutes. After cooling to 70°C under pressure, the molded test bars were removed.

During the curing cycle, excess resin was squeezed out, yielding a final composite composition of 35% (by volume) resin content.

d. Resin Specimen Preparation

Test specimens prepared from neat resin were obtained by pouring the prepared resin (as above) into a glass mold preheated to 150°C. The glass mold was fashioned from two glass plates, sprayed with mold release agent, which were separated on three sides by a 0.25 in. silicone rubber gasket. The glass plates were clamped from the outside for the gasket to form a tight seal. The resin was introduced through the open fourth side of the mold. The curing schedule was

identical to that of the composite samples. Specimen were cut from the resin plate with a water-cooled diamond blade saw at a speed of 0.5 in./min.

2. SURFACE AREA AND POROSITY

Fibers used in this work were characterized by mercury porosimetry and by nitrogen adsorption. Both methods show that the fiber surfaces are very low in porosity (less than about 10^{-4} cm^3/gram). The surface area of ST-fiber was slightly more than twice that of the GR-type fiber.

The mercury intrusion measurements were performed with an Aminco porosimeter, at pressures up to 50,000 psig. The sensitivity of the method is only marginal for this purpose, but increments of porosity with increasing pressure of the order of 2×10^{-4} cm^3/gram could be detected with fair confidence. While substantial effects were noted in the 1000Å range, corresponding to gross surface features of the fibers, practically nothing was visible between 30 and 300Å for either treated or untreated fibers.

Nitrogen adsorption experiments were performed by the dynamic desorption technique, using a Quantasorb instrument at the boiling point of liquid nitrogen. The relatively low specific surface area of these fibers made such measurements quite difficult, especially at high partial pressures; the values obtained at p/po = 0.9 are felt to be especially unreliable.

The nitrogen adsorption data have been tabulated in Table III, together with specific surface areas calculated by two methods: the conventional BET method and the t-plot approach of Lippens and deBoer (Reference 29). The values obtained by the two methods agree quite well.

It should be noted that the application of both these methods to graphitized carbon surfaces has been the subject of some discussion and criticism (Reference 30,31). However, they seem to provide, in this case at least, a uniform interpretation of all the data. The BET plot (p/p_o from 0.05 to 0.2) is shown in Figure 1, the t-plot (p/p_o from 0.2 to 0.9) is given in Figure 2. For reasons discussed by Pierce, the points at p/p_o = 0.2 and 0.3, while shown in Figure 2, were not used in the calculation of areas by the t-plot method. As mentioned above, the points at p/p_o = 0.9 were also given little weight. The parameters used in constructing the t-plot were those proposed by Lippens and deBoer, rather than those advocated by Pierce, which seemed to fit the experimental data rather poorly.

The t-plot is especially useful as a means of detecting microporosity, which is indicated by a more or less sudden change to a line of lesser slope. The lines in Figure 2 are open to this interpretation. To obtain an idea of the maximum microporosity which might be present, the alternative dotted line was drawn through the points of the upper curve (the ST-fiber). The intercept of this line on the Y-axis is 0.05 cm^3 (STP)/gram; it appears to "bend over" around t=2,

TABLE III

NITROGEN ADSORPTION DATA FOR GRAPHITE FIBERS

P/P_o	$t^{(1)}$	N_2 Adsorption - cc (STP)/gram	
		GR-3-152-01	ST-3-152-04
0.0509	-	0.0558	0.140
0.1015	-	0.0725	0.165
0.200	1.23	0.0910	0.200
0.300	1.42	0.106	0.230
0.400	1.61	0.123	0.270
0.500	1.83	0.140	0.310
0.600	2.08	0.163	0.368
0.700	2.42	0.195	0.421
0.800	2.98	0.241	0.507
0.900	4.22	0.326	0.699.

Note:

(1) Number of monolayers, according to Pierce, (Reference 31).

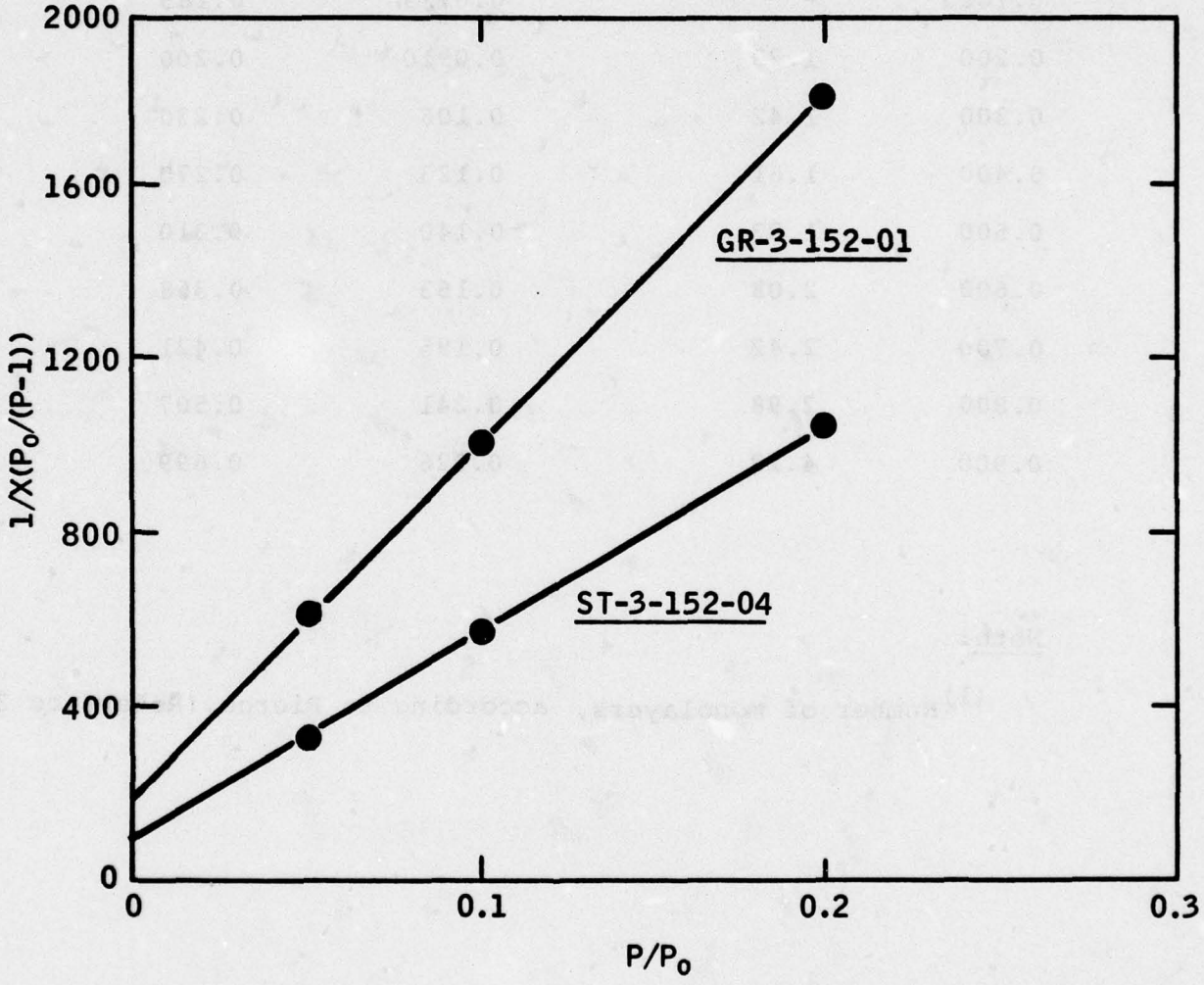

Figure 1. Surface Area of Untreated (GR) and Surface Oxidized (ST) Graphite Fibers (BET-Plot).

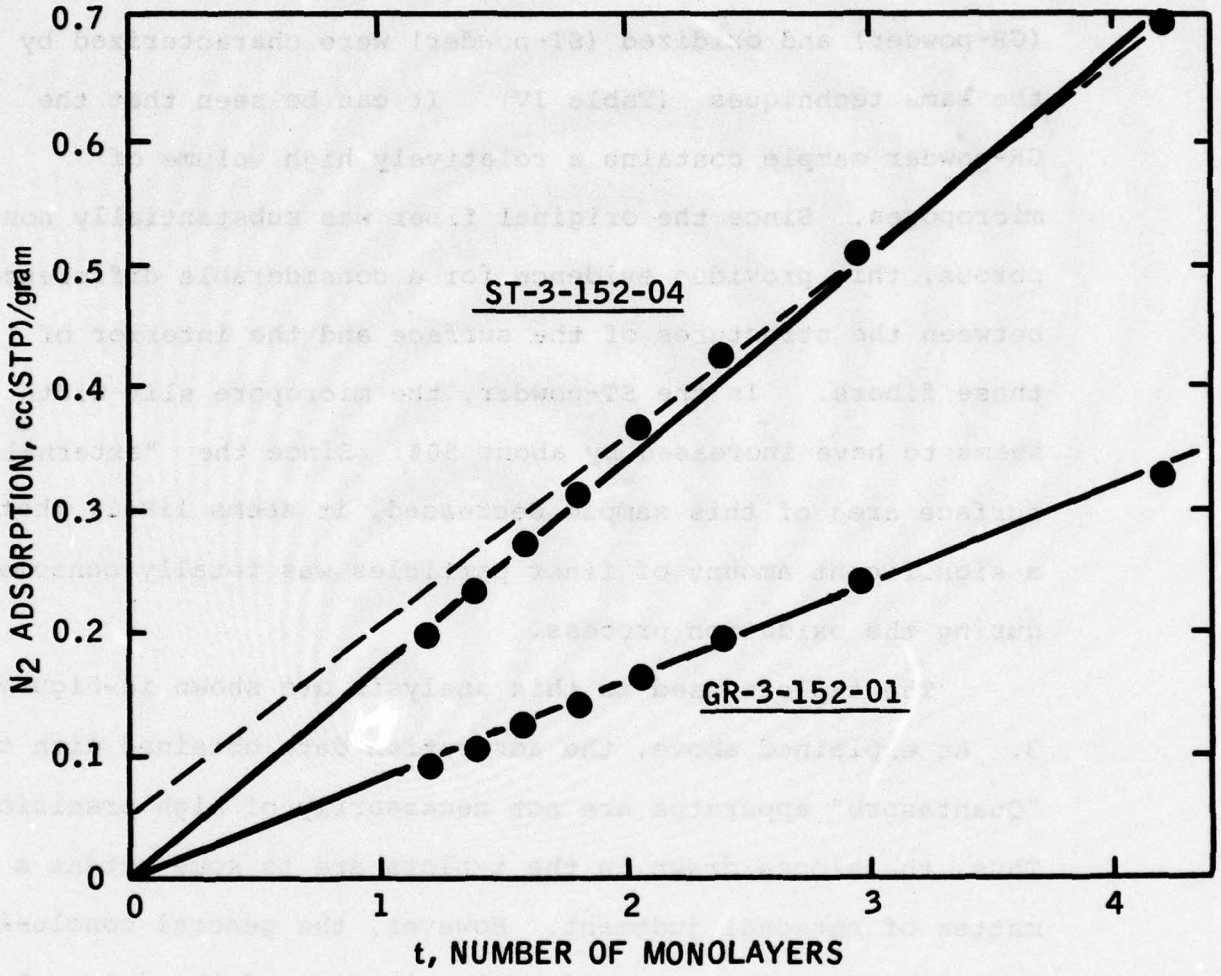

Figure 2. Surface Area of Graphite Fibers of Figure 1 (t-Plot).

corresponding to a layer of adsorbed N_2 about 7Å thick. Assuming slit micropores, this would amount to a micropore volume of about 7×10^{-5} cm^3/gram, containing about $0.1 m^2$/gram of surface area, as an upper limit.

Samples of cryo-milled graphite fibers, unoxidized (GR-powder) and oxidized (ST-powder) were characterized by the same techniques (Table IV). It can be seen that the GR-powder sample contains a relatively high volume of micropores. Since the original fiber was substantially non-porous, this provides evidence for a considerable difference between the structures of the surface and the interior of these fibers. In the ST-powder, the micropore slit width seems to have increased by about 50%. Since the "external" surface area of this sample decreased, it seems likely that a significant amount of finer particles was totally consumed during the oxidation process.

The t-plots used in this analysis are shown in Figure 3. As explained above, the adsorption data obtained with the "Quantasorb" apparatus are not necessarily of high precision Thus, the slopes drawn in the t-plots are to some extent a matter of personal judgment. However, the general conclusions just stated seem to be reasonable, in view of the data. A comparison of surface area data for the various samples is compiled in Table V.

TABLE IV

NITROGEN ADSORPTION DATA FOR CYRO-MILLED FIBERS

P/P_o	$t^{(1)}$	N_2 Adsoprtion - cc(STP)/gm. cryo-milled	cryo-milled/oxidized
0.200	1.23	10.43	6.96
0.300	1.42	11.12	7.99
0.400	1.61	12.50	9.00
0.500	1.83	13.80	9.36
0.600	2.08	14.24	10.42
0.700	2.42	15.37	11.38
0.800	2.98	17.44	12.75
0.850	3.46	19.10	13.63
0.900	4.22	21.96	14.43
0.950	5.25	24.00	16.22

Note: $^{(1)}$See Table III

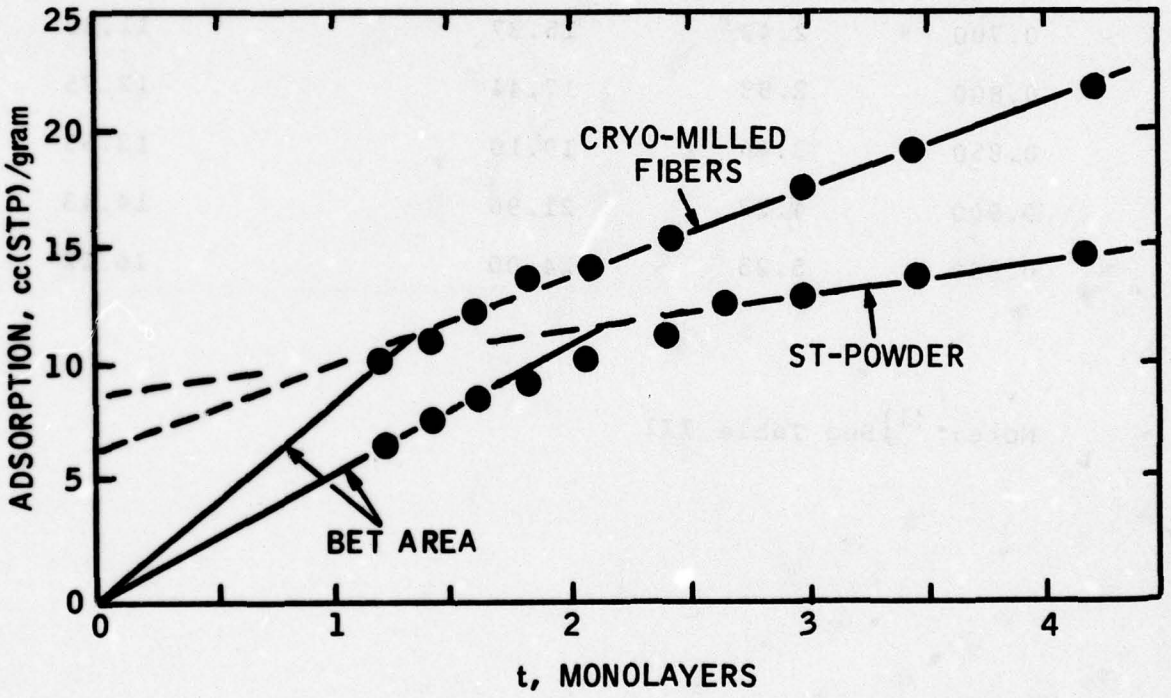

Figure 3. Surface Area of Cryo-Milled and Cryo-Milled/Oxidized Graphite Fiber. (ST-Powder)

TABLE V

COMPARISON OF SURFACE AREA DATA FOR GRAPHITE FIBERS AND POWDERS

	GR-Fiber	ST-Fiber	GR-Powder	ST-Powder
Surface Area (BET), m^2/gm	0.345	0.737	35.9	24.0
Surface Area (t-plot), m^2/gm	0.340	0.745	15.9	5.8
Micropore Area, m^2/gm [1]	-	< 0.1	20.1	18.2
Micropore Volume, cm^3/gm	-	$< 7 \times 10^{-5}$	1.01×10^{-2}	1.38×10^{-2}
Average Pore Width ($\overset{\circ}{A}$)	-	7	10.1	15.2

[1] Calculated from micropore volume and width, for slit micropores.

3. SURFACE REACTIONS (TAGGING)

ST and GR-type fibers, and ST-type powder, were reacted with epibromohydrin (I).

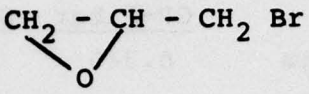

(I)

The epibromohydrin was expected to react with functional groups at the surface of the solids, forming esters (II) with pendant carboxyl groups and ethers (III) with pendant hydroxyl groups.

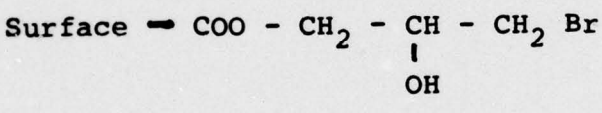

(II)

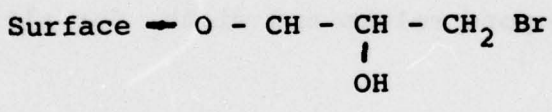

(III)

Reactive sites at the surface thus tagged contain a bromine atom which was used for determination of the concentration of these sites by ESCA and NAA (see below).

THe tagging reaction was carried out in a heavy walled test tube sealed with a Teflon stopper via metal screw couplings (Aerosol Test Bottle, A. H. Thomas, 1976 Catalogue p. 147, No. 1769-D12). The tube and stopper were predried in

vacuo at 85°C for two hours. Samples to be tagged, either as a fiber of about five inch length, or as a powder, were washed with acetone to remove surface contaminants, followed by drying in vacuo at 85°C for two hours. Three grams of the sample were added to the tube, 5 ml. of epibromohydrin (Eastman) introduced via a syringe, and the tube sealed. After 24 hours at 150°C, the tagged material was washed with acetone and dried in vacuo at 85°C for one hour.

The same conditions were employed for tagging surface sites with 3,5- dinitrobenzoyl chloride (Aldrich Chemical Company)

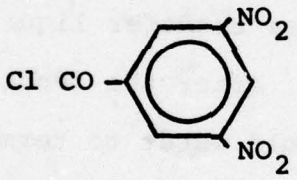

(IV)

This acid chloride is specific for phenolic-type surface groups, forming an ester (V) which contains two nitrogen atoms per tagged group.

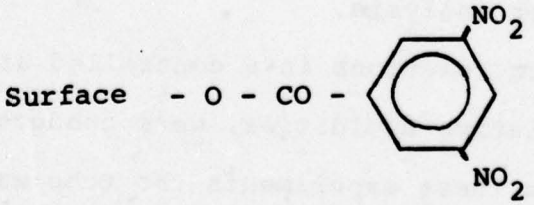

(V)

The nitrogen atoms were used for the determination of these sites by ESCA (see below). Since the acid chloride is a material of m.p. 69-71°C, it was added as a solid. Care was

taken to ensure that the melt of the acid chloride, which is formed during the reaction at 150°C, contacted the sample to be tagged.

4. DETERMINATION OF DEGRADATION KINETICS OF TAGGED SURFACE GROUPS

Reaction conditions for the degradation experiments were established by initial screening experiments. In these, Aerosol Test Bottles (see Surface Reactions) were employed. The tagged sample (500 mg) was placed into the tube, 10 ml of water was added, and the sealed tube exposed to the desired temperature in an Akiba constant temperature bath (propylene glycol as transfer liquid, ± 0.05°C max. temperature variation). After the reaction period, the tube was submerged in cold water to terminate the degradation reaction. The tube was opened immediately, the sample was transferred to a filter, and washed exhaustively with acetone. After air drying for two hours, the sample was dried in vacuo for two hours at 85°C, then sealed in a vial and kept for analysis.

Degradation reactions in a controlled atmosphere, i.e. at different relative humidities, were conducted in the same system. In these experiments the tube was predried in vacuo for two hours at 85°C, with the sample contained in the tube. The desired amount of water (distilled) was added to the tube via a calibrated glass capillary (Disposable

Micro-Sampling Pipets, A. H. Thomas, Cat. No. 8206) while still hot. The tube was sealed immediately and treated as described above.

For the determination of the degradation kinetics a different reaction vessel was adopted which had the advantage of having a smaller mass and, therefore, reached the desired reaction temperature more rapidly than the high-mass Aerosol Test Bottles. The reaction vessel was fashioned from a 9 in. long glass pipet (Fischer Brand®, Catalogue 74, p. 633, No. 1367853) by sealing the capillary end. Into this tube was added 400 mg of tagged material and 500 µl of distilled water (for hydrolysis experiments at 100% R_H) or no water (for thermolysis at 0% R_H). The pipet was then sealed at the necked end, yielding a tube of ca. 100 mm (4 in.) in length, and of ca. 7 mm O.D. (4 mm I.D.). The reaction was carried out as described above. Isolation of the samples and preparation for analysis was also done in the same manner.

5. INSTRUMENTAL ANALYSES

a. Neutron Activation Analysis (NAA)

Samples generated in this work were sent for NAA to General Activation Analysis, Inc., San Diego, California. The bromine in tagged specimens, before and after degradation, was determined by irradiation for 30 minutes in a TRIGA Mark I Nuclear Reactor at a flux of 1.8×10^{-2} n/cm^2-sec.

After a decay of two days, it was counted on a Ge(Li) detector coupled to a multi-channel gamma-ray spectrometer. The element bromine produced Br-82 with a half-life of 1.5 days. The results were reported in ppm bromine contained in the specimen.

b. Induced Electron Emission Analysis (ESCA)

Analyses were performed with a Varian IEE-15 Induced Electron Emission Spectrometer, using a high intensity magnesium anode X-ray source. Normal anode settings were 10 kV and 0.15A. The vacuum was maintained at 1×10^{-6} Torr by means of a titanium sublimation pump. Fiber samples were mounted on a double-faced tape on a cylindrical holder yielding a surface area of about 6 cm^2. Powder samples were mounted in the same manner.

c. Vacuum Pyrolysis/Mass Spectroscopy (VPy/MS)

The objective of this segment of work was to obtain information about the type and stability of surface groups on graphite fiber and graphite fiber powder, before and after oxidative treatment.

Experiments were carried out in a quartz tube (2.5 cm O.D., 15 cm long) which was directly attached to the sample inlet of an AEI MS-902 double-focusing instrument via Kovar seals and a VCR® Vacuum coupling (Cajon Comp., Cleveland,

Ohio). The tube was horizontally positioned in a Lindberg furnace. The temperature of heating was controlled through a programmed voltage rise by a converted gas chromatography temperature programmer at a nominal 6°C/min program rate. A record of the actual temperature rise with time, measured at the surface of the quartz tube in the furnace, is shown in Figure 4. It indicates that the total heat-up cycle to 1000°C required about 90 minutes. During this period of time the atmosphere of the degrading sample was continuously exposed to the MS instrument and sampled at 20°C furnace temperature intervals. Prior to the degradation experiment, the quartz tube was precleaned by heating to 1000°C at 10^{-7} Torr.

A single vacuum pyrolysis experiment encompassed three heat-up cycles during which gas evolution data were collected. On "day 1" the tube with the sample was heated to 1000°C at 10^{-7} Torr, followed by cooling in vacuum and standing over night for 12 hours. On "day 2" the cycle was repeated. After cooling the tube, the sample was exposed to air for 12 hrs. through the MS instrument. On "day 3" the tube was evacuated to 10^{-7} Torr and then reheated to 1000°C.

Thus, the gas evolution measured on "day 1" represented adsorbed and chemisorbed products from the sample and quartz tube wall. Data collected on "day 2" were indicative of products formed by a reaction between sample and background atmosphere at 10^{-7} Torr. Finally, the gas phase sampled on "day 3" is a measure of effects introduced by the air atmosphere

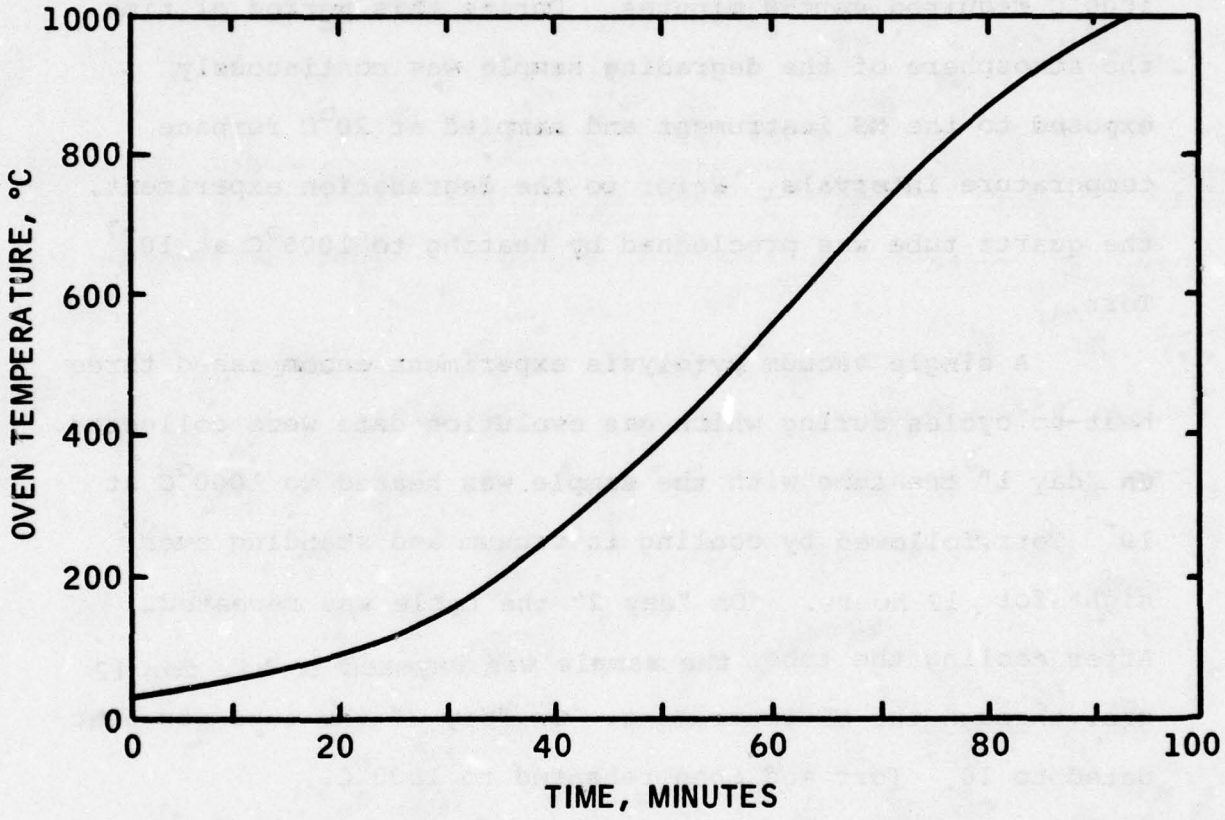

Figure 4. Heating Rate of Vacuum Pyrolysis Furnace.

adsorbed on sample and glass wall, plus the interaction effects between sample and background oxygen as seen on "day 1". Figure 5 depicts the oxygen background on "day 2" and "day 3". As seen, it rapidly commences to decrease above 250°C and diminishes to about 5% of the room temperature background concentration at 600°C, indicating a reaction with the substrate of increasing severity in this temperature interval. Above 600°C essentially all of the background oxygen has reacted with the substrate.

Figures 6 and 7 summarize the results of the CO_2 and water evolution measurements, respectively. Amounts are plotted in terms of raw intensity. The evolution of CO was not measured in these experiments since it required an alternate detection system.

Figure 6 shows a trimodal distribution for the CO_2 evolution, peaking at 300°C, 360°C, and 525°C. The 360°C peak vanishes after deduction of data from "day 3". The remaining bimodal curve suggests the presence of two distinct types of CO_2 producing surface groups of different thermal stability.

The water evolution, as given by Figure 7, exhibits a more complex behavior. It shows a trimodal distribution with a major peak at 210°C, and two minor peaks at 450°C and 640°C, none of which vanishes after the background correction for "day 3" is made.

By comparison, it is interesting to note that J. S. Perkins (Reference 22) has reported for Thornel 50 a trimodal CO_2

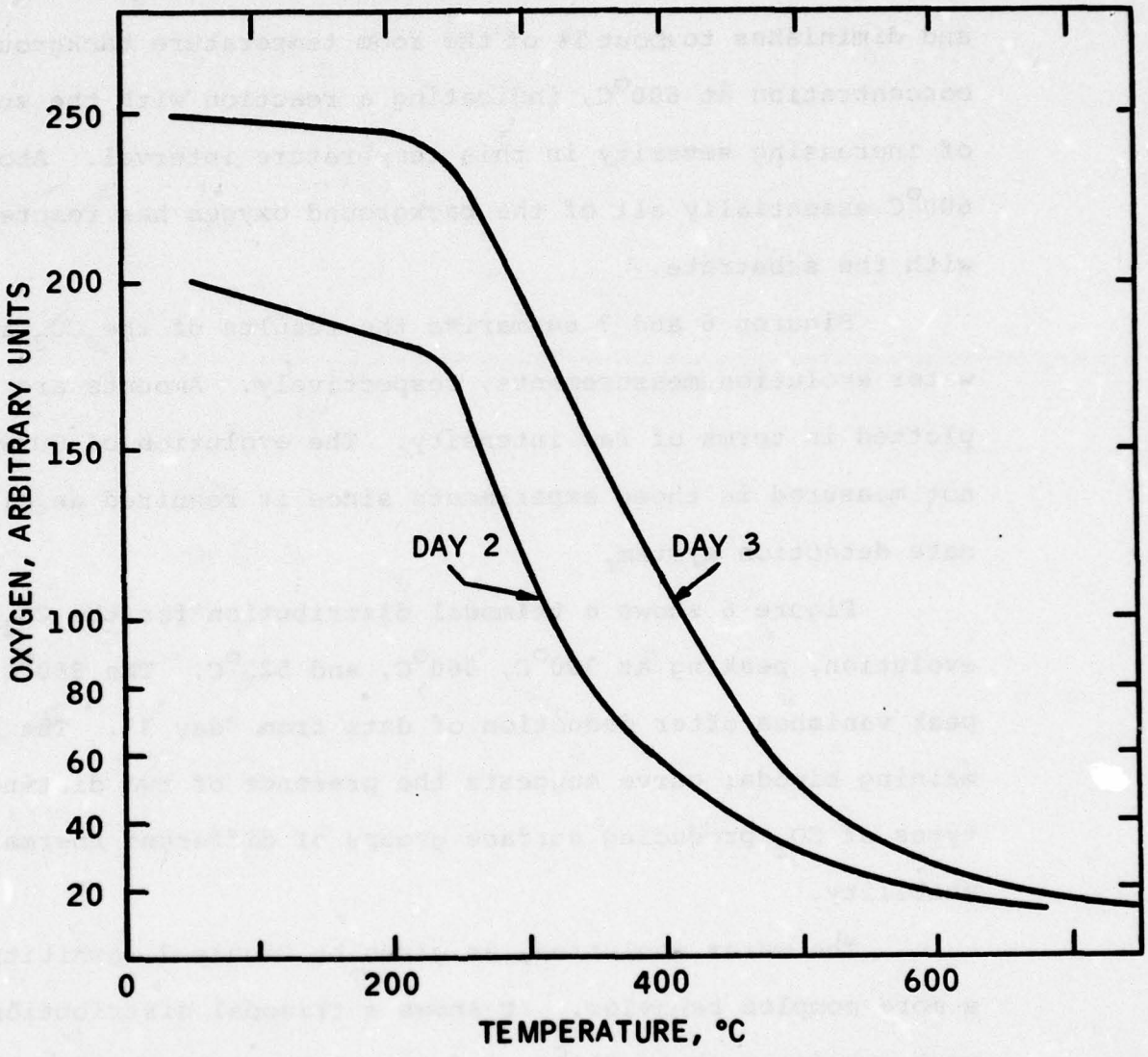

Figure 5. Typical Oxygen Background in Vacuum Pyrolysis/Mass Spectrometry Experiments.

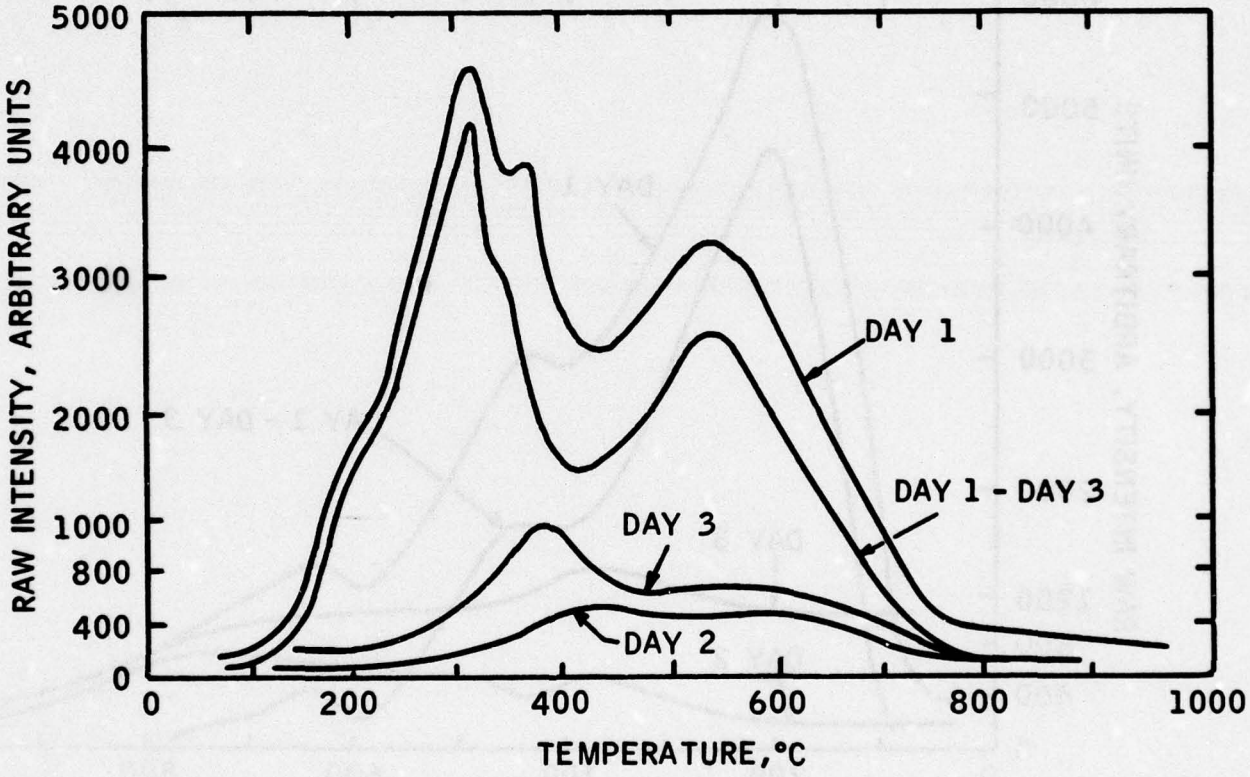

Figure 6. CO_2 Evolution of ST-Fiber in Vacuum Pyrolysis/Mass Spectrometry. (Low Resolution Run)

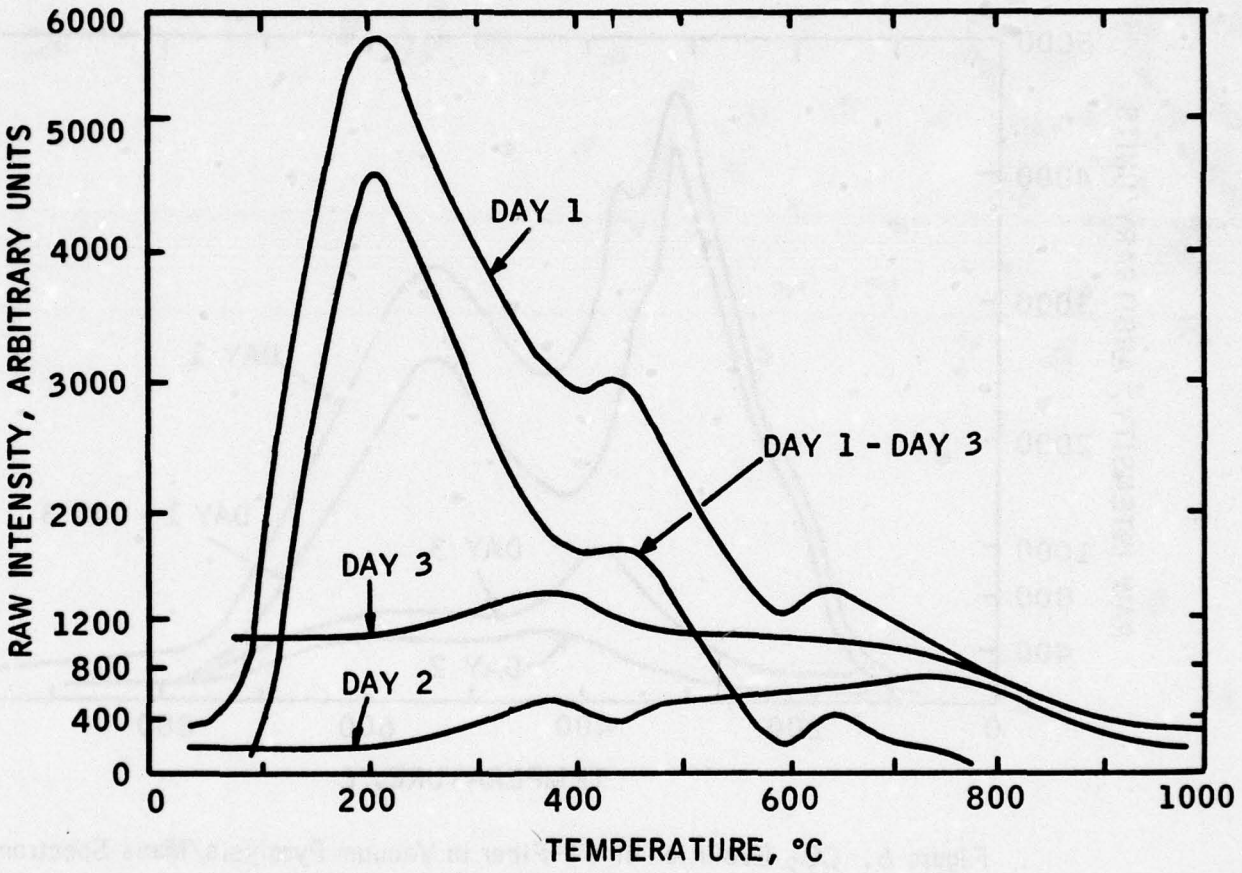

Figure 7. Water Evolution of ST-Fiber in Vacuum Pyrolysis/Mass Spectroscopy. (Low Resolution Run)

evolution profile peaking at 240°C, 400°C and 550°C and T. Fort (Reference 21) a bimodal CO_2 profile peaking at 300°C and 680°C, and a single peak for H_2O at 330°C.

The CO evolution profile of ST-Fiber was obtained by a high resolution technique. In order to provide an internal standard, the CO_2 profile was determined simultaneously. Figure 8 shows the results of the high resolution analysis of CO and CO_2 for ST-Fiber for day 1. Data collected on Day 2 indicated the absence of a reaction between sample and background atmosphere at 10^{-7} Torr. Hence, the day 3 experiment was omitted. Data in Figure 8 are plotted in terms of raw intensities from galvanometer readings.

The reproducibility of results is shown in Figure 9 which compares the CO_2 profiles obtained in the high resolution experiment with the previously reported low resolution experiment. Again, peak heights are recorded in terms of raw intensities without correction to sample size. As is apparent from this comparison, the reproducibility of data is quite good. A slight discrepancy is noticeable beginning at about 400°C indicating that the temperature program was not completely identical between the two runs and led to a shift of the previously recorded second major CO_2 evolution peak from 530°C to 500°C. It will be noted that the 360°C peak of the day 1 low resolution experiment (Figure 6) which vanished after connection for day 3 evolution, does not appear in the high resolution experiments on day 1. This confirms that the 360°C

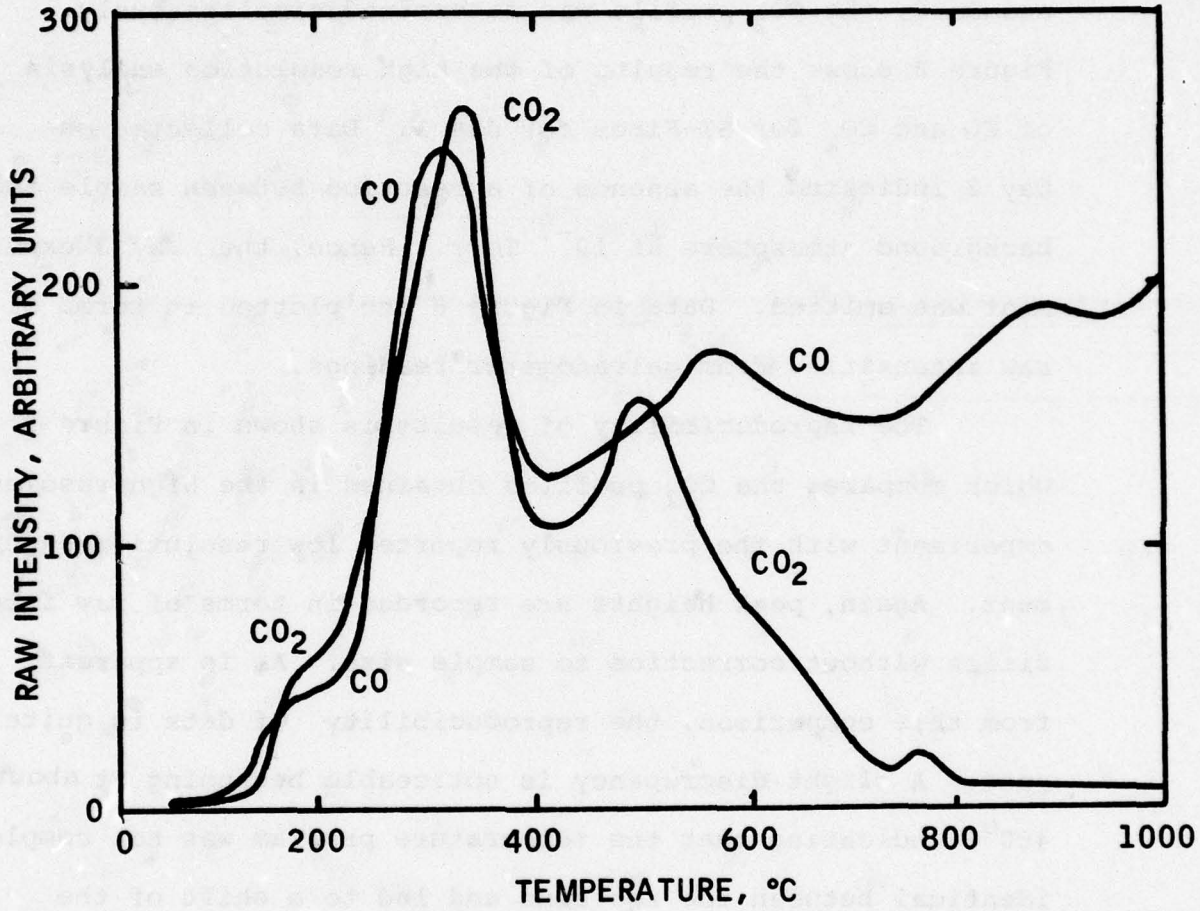

Figure 8. CO & CO_2 Evolution of ST-Fiber in Vacuum Pyrolysis/Mass Spectrometry. (High Resolution Run)

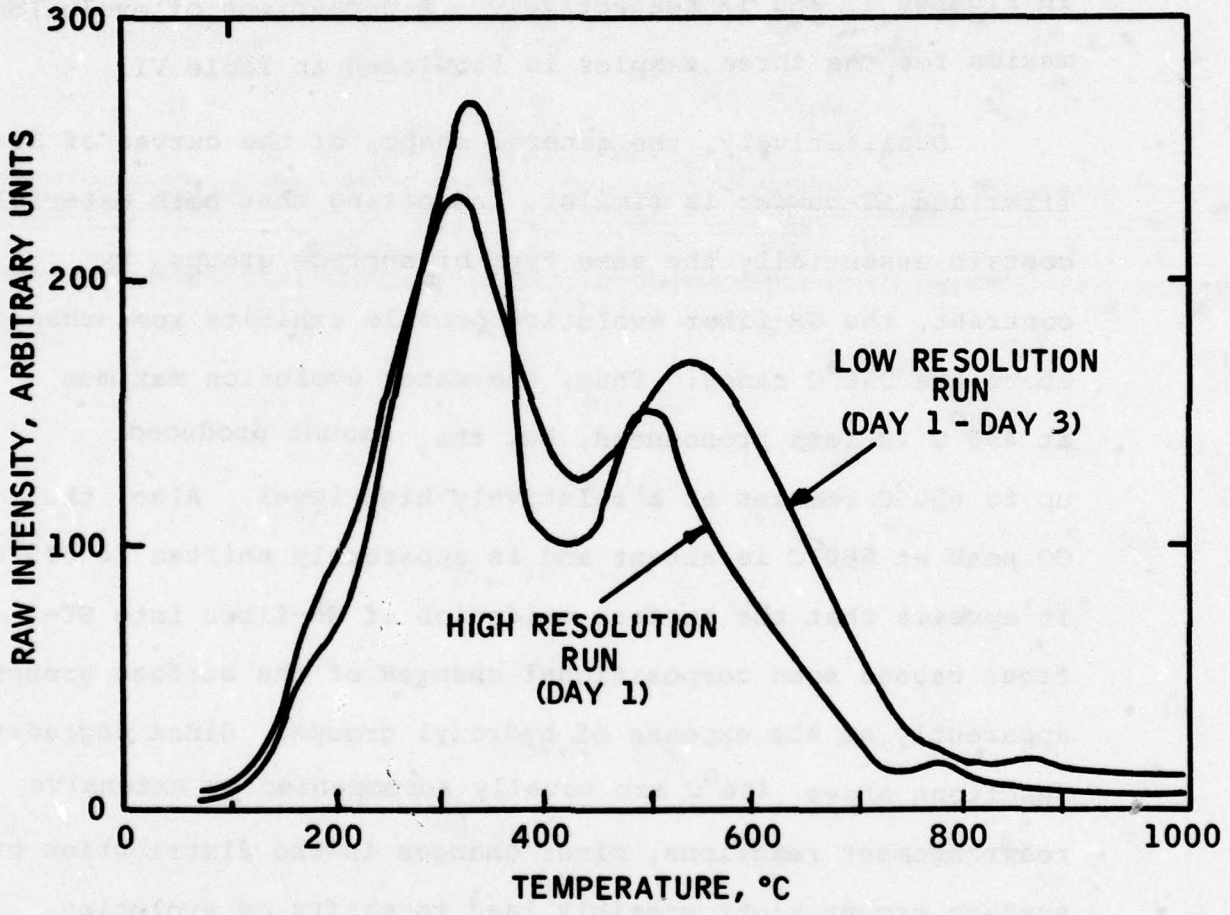

Figure 9. Comparison of CO_2 Evolution Data of ST-Fiber in Vacuum Pyrolysis/Mass Spectroscopy.

peak was caused by an interaction reaction and establishes the bimodal evolution profile of CO_2.

The evolution profiles of CO, CO_2, and H_2O for ST-fiber are shown in Figure 10. The intensity scale has been now normalized to galvanometer calibration. Corresponding evolution curves for GR-fiber and for ST-powder are recorded in Figures 11 and 12 respectively. A comparison of evolution maxima for the three samples is tabulated in Table VI.

Qualitatively, the general shapes of the curves of ST-fiber and ST-powder is similar, indicating that both materials contain essentially the same type of surface groups. By contrast, the GR-fiber evolution profile exhibits some changes above the 350°C range. Thus, the water evolution maximum at 450°C is less pronounced, but the amount produced up to 650°C remains at a relatively high level. Also the CO peak at 560°C is absent and is apparently shifted to 675°C. It appears that the surface oxidation of GR-fiber into ST-fiber causes some compositional changes of the surface groups, apparently at the expense of hydroxyl groups. Since degradation reactions above 400°C are usually accompanied by extensive rearrangement reactions, minor changes in the distribution of surface groups might possibly lead to shifts of evolution maxima in the high temperature region. Hence, in the absence of additional data, it is difficult to draw any further conclusion as to the finer details of the structure of surface groups. In rationalizing the gas evolution profiles, it is

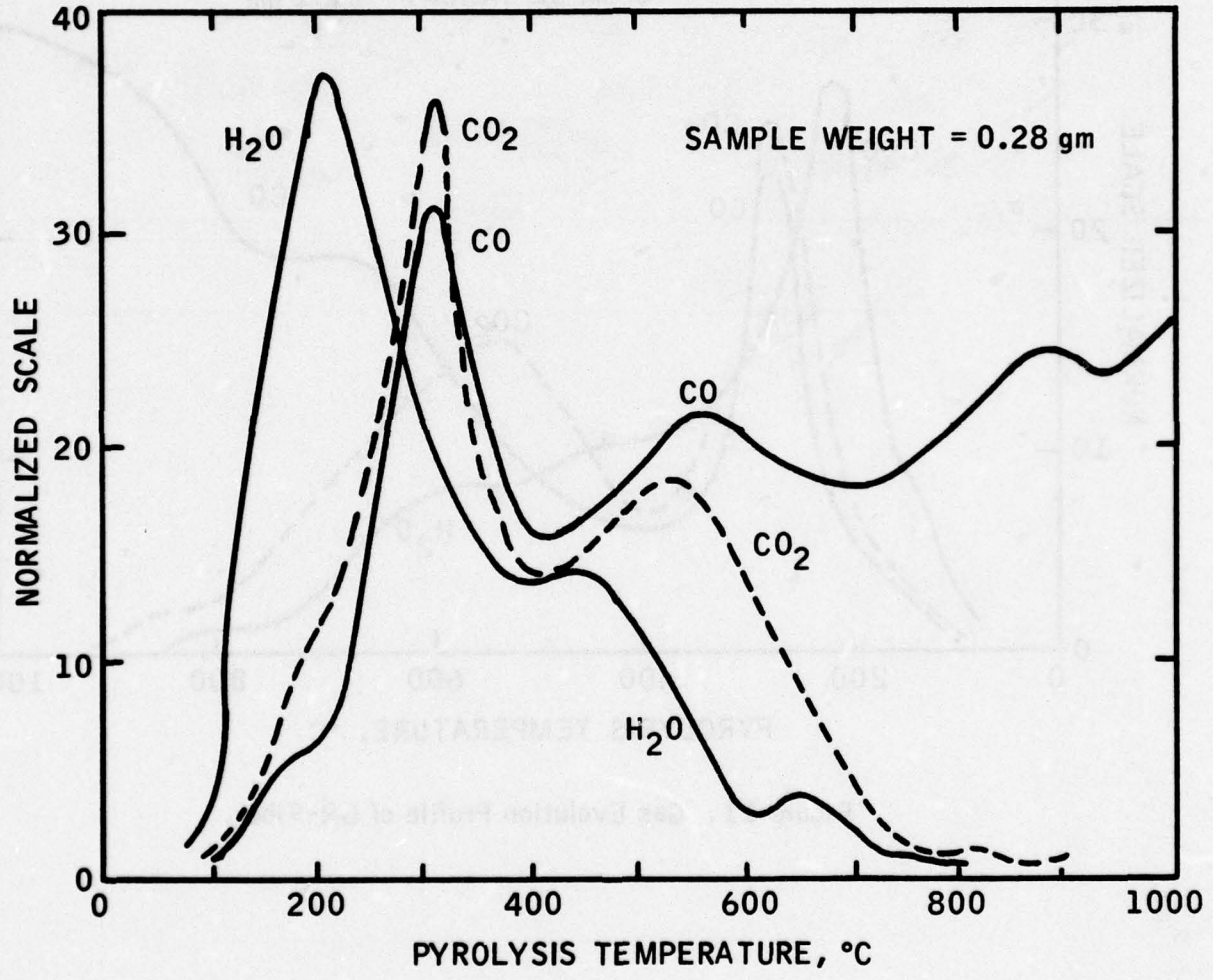

Figure 10. Gas Evolution Profile of ST-Fiber.

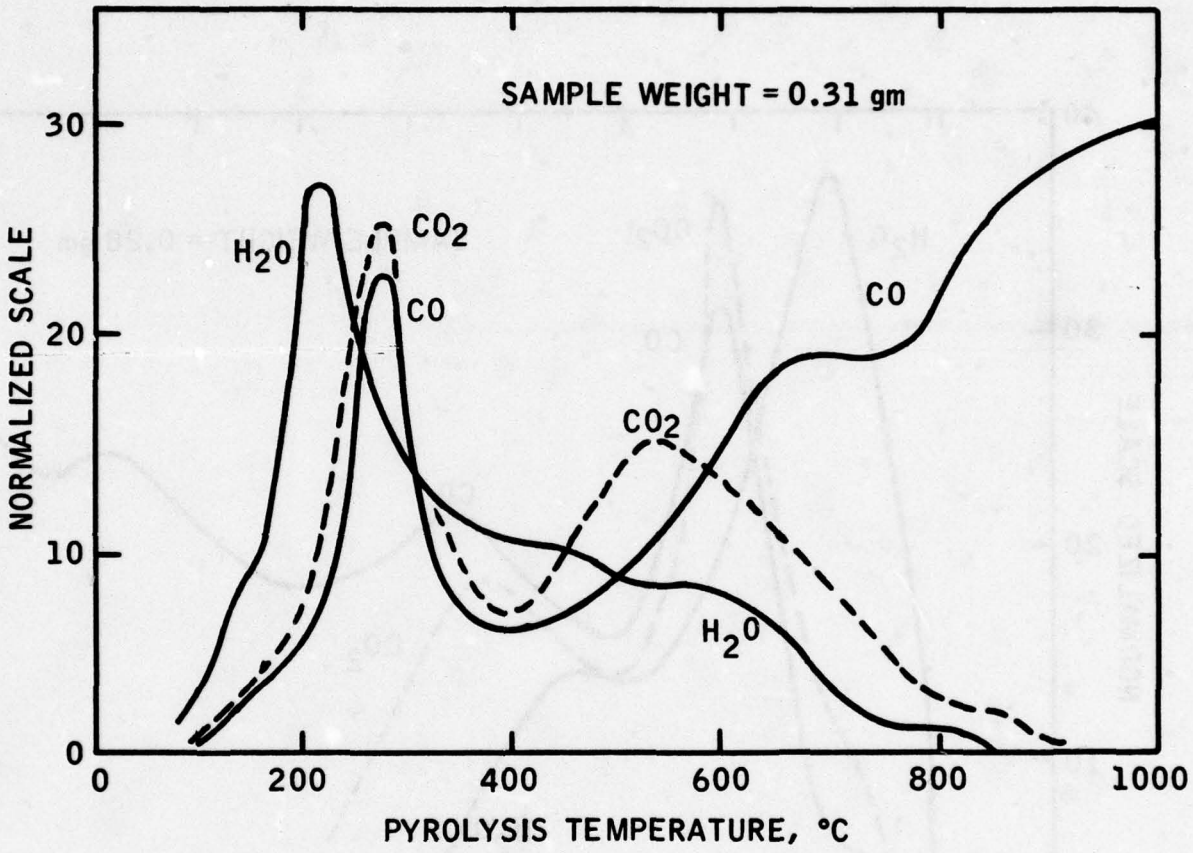

Figure 11. Gas Evolution Profile of GR-Fiber.

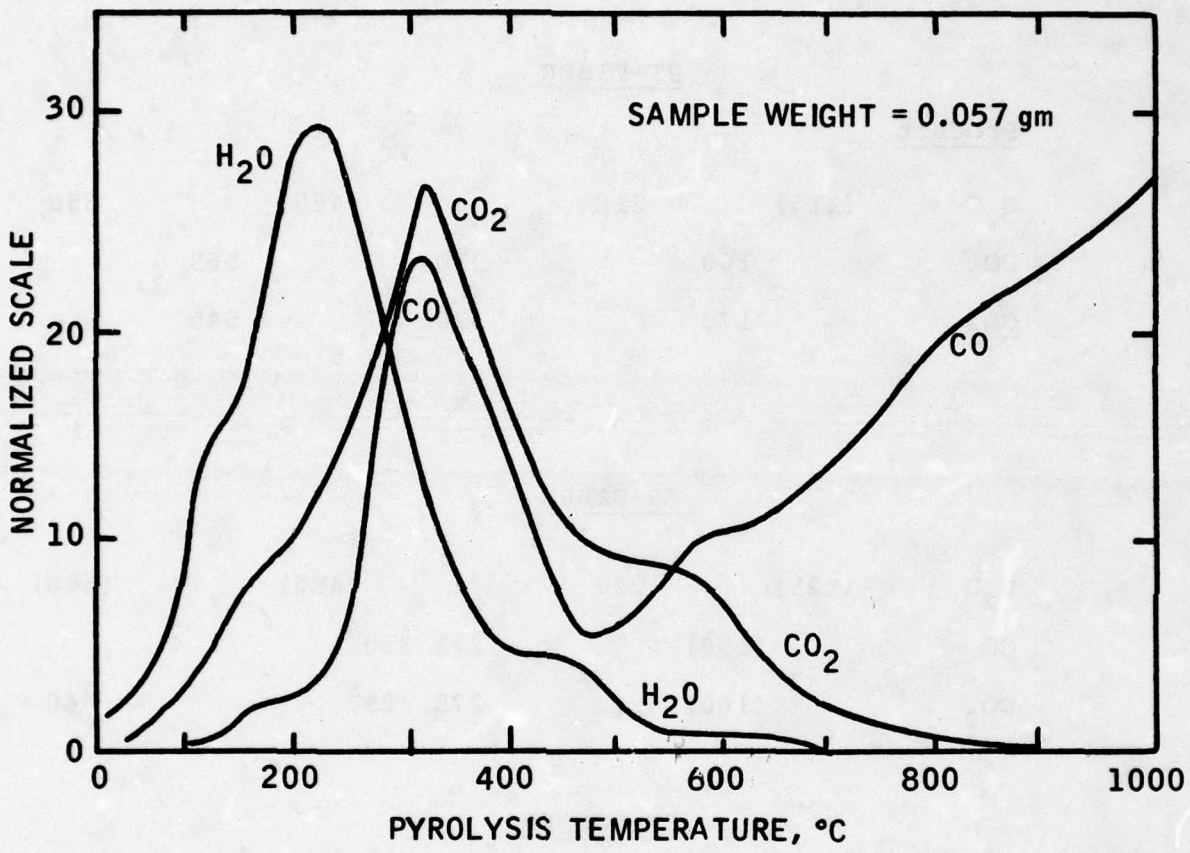

Figure 12. Gas Evolution Profile of ST-Powder.

TABLE VI

TEMPERATURES OF EVOLUTION MAXIMA

ST-FIBER

Product	°C									
H_2O	(115)		210			450			650	
CO		160			310			565		860
CO_2		170			320			545		

GR-FIBER

H_2O	(125)		220			(450)			(580)	
CO		(150)			275	330^S				675
CO_2		(160)			275	325^S			540	

ST-POWDER

H_2O	(120)		210			440			(650)	
CO		165^S			320			560		850
CO_2		175^S			325			540		

Temperatures in paranthesis indicate weak maxima;
S indicates a shoulder on a maximum peak.

reasonable to assume that the low temperature maxima of CO (160°C) and CO_2 (170°C) represent amounts of these gases which are physically adsorbed on the fiber while the corresponding water peak appears as an unresolved shoulder near 110°C. The first water maximum (210°C) seems to be caused by chemisorbed species probably held in the matrix by hydrogen bonding. The evolution maxima of CO and CO_2 in the 300°C region occur simultaneously, while H_2O evolution in this region is still quite strong. This suggests a complex reaction between pendant carboxyl groups of the dicarboxylic type (I) to anhydrides(II), or pendant hydroxyl/carboxyl group combinations (III), to lactones (IV),

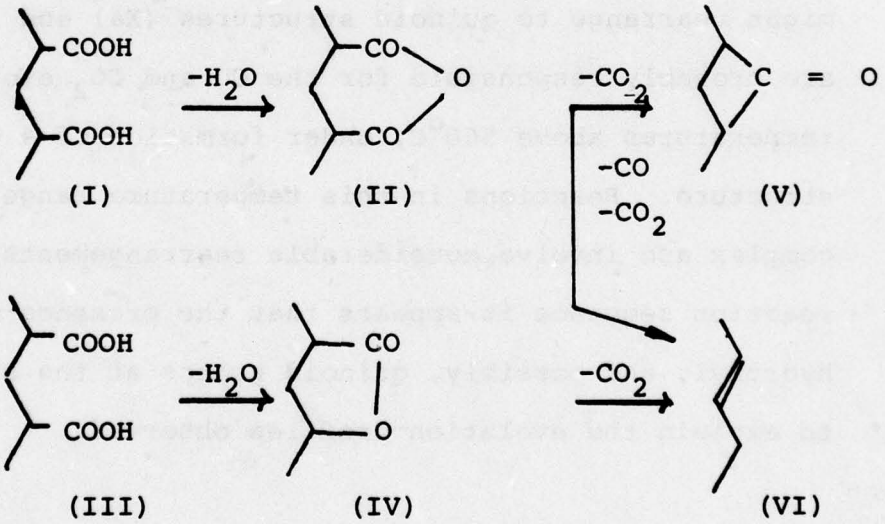

whereby the anhydride could lose CO to form a highly temperature stable cyclic ketone (quinone V), and the lactone form

a graphitic structure (VI) under loss of CO_2. Any neighboring hydroxyl groupings (VII), or quinone/hydroxyl combinations (VIII), would loose water at higher temperatures (450°C) to form cyclic ethers (IX) which

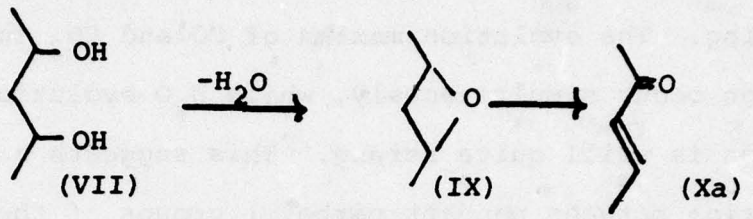

(VII) (IX) (Xa)

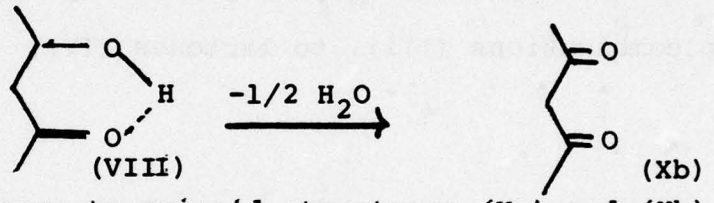

(VIII) (Xb)

might rearrange to quinoid structures (Xa) and (Xb). These are probably responsible for the CO and CO_2 evolution at temperatures above 560°C, under formation of a graphitic structure. Reactions in this temperature range are probably complex and involve considerable rearrangements. From this reaction sequence it appears that the presence of carboxyl, hydroxyl, and possibly, quinoid groups at the surface suffice to explain the evolution profiles observed.

d. Pyrolysis/Gas Chromatography (Py/MS)

The objective of this section was to obtain data supportive to VPy/MS experiments. In contrast to the latter, pyrolysis/GC was hoped to permit quantification of the total amount of the various gases desorbed from the graphitic surface.

Several problems were encountered in the use of the pyroprobe, mostly traceable to the high temperatures required with graphite fibers to liberate all oxygenated species. As has been noted in the literature, commercially available pyroprobes do not yield a homogeneous temperature region across the sample to be pyrolized. Also, automatically set firing times are apparently too short for complete degradation to volatile products. Based on a short investigation of these problems, the instrument was modified to allow manual control of the firing time and to give better uniformity of the temperature zone. Results obtained indicated that for total desorption at 1000°C, a firing time of 15 minutes was required.

The primary species to be determined by this method were CO and CO_2 which are the main degradation products of the oxygenated groups at the graphite surface. The CO_2 level may be considered a rough measure of carboxyl groups which are capable of reacting with epoxy moities. This measure is, however, a minimum estimate at best, since the secondary reaction $CO_2 + C \longrightarrow 2CO$ exhibits a significant rate at 1000°C, even at the short residence times employed during the pyrolysis.

The Py/GS system was calibrated with a certified CO/CO_2 mixture in helium. Peak areas were obtained by electronic integration with a dedicated computer (PACE® system, EAI).

Least square analysis of data yielded,

$$CO\ (gm) = 9.30 \times 10^{-8} + w.70 \times 10^{-3}\ AREA$$

$$CO_2(gm) = 7.10 \times 10^{-7} + 2.74 \times 10^{-3}\ AREA$$

with indices of determination equal to 0.999 and 0.994, respectively.

From these equations the amount of gases evolved from the master batch sample of ST-powder was computed as

1.377 mg CO/gm powder (40μmol/gm)

and

0.549 mg CO_2/gm powder (12μmol/gm)

Because of the physical limitations in sample size, the GC peaks obtained by the pyrolysis of ST-fibers were small and could not be measured accurately by the PACE computer. However, the ratio of CO/OC_2 peak heights, determined from recorded curves of ST-fiber sample pyrolysis appeared to be the same as the ratio of peak areas measured by the PACE computer on powder pyrolysis, i.e., ca. 2.2. Further, it was estimated that the amount of gases evolved from the ST-powder was some 12 times larger than from the ST-fiber.

By contrast, graphical integration of the VPy/Ms

curves of Figures 10, 11 and 12, yielded CO/CO_2 ratios of 1.95 (ST-Fiber), 1.79 (GR-Fiber) and 1.66 (ST-Powder), and, further, a ratio of 1.43/1/3.7 for the total amount of $CO + CO_2$ evolved from ST-fiber/GR-fiber/ST-powder, respectively. It is obvious that the precision of measurements expected from the Py/GC method was not attained. These poor results originate probably in the incomplete heating of the sample in the pyroprobe, the small sample size which was accepted by the pyroprobe, and the commensurately high inaccuracy of the gas chromatographic curves recorded. It will also be noted that the total amount of $CO + CO_2$ found in the Py/GC measurements is less than the actually tagged carboxyl groups (see Table XIV, Discussion Section), i.e. 62 vs. 80 μmole, respectively.

Considerably more work would have had to be done to resolve these problems. In view of the results obtained in the other segments of work, the PY/GC activity was terminated.

SECTION III
DISCUSSION

1. INDUCED ELECTRON EMISSION MEASUREMENTS (ESCA) ON TAGGED GRAPHITE FIBER SUBSTRATES

ESCA runs on GR-and ST-fibers revealed no differences between these samples. A large oxygen signal was measured (ca.4%) possibly indicating the presence of functional groups but more probably simply residual water.Although samples were degassed in the instrument at $5 - 7 \times 10^{-7}$ Torr, this treatment was probably not sufficient to remove residual moisture. No Br interference lines were detected, and Na and Cl were each less than 0.1% relative to C.

The analysis of epibromohydrin (EBH) tagged samples showed the presence of bromine in both types of fibers, with the ST-sample exhibiting about a four fold higher level than the GR-sample. After EBH treatment there was a significant oxygen increase on both samples with more oxygen on the ST-fiber. This oxygen increase was not one to one with bromine as the EBH reaction should have provided. Rather, there was excess oxygen, suggesting that water could be clustering on the hydroxyl group of the reacted EBH, i.e.,

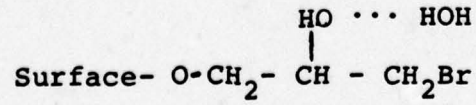

whose hydrogen bonding was sufficiently strong to prevent desorption under the conditions of the measurements. Drying experiments on composite samples (see below) showed that the removal of residual moisture occurs slowly even at elevated temperature in vacuo, corroborating the potential hydrophilicity of the epoxidized surface. Conversely, it might be expected that dried fiber samples would rapidly re-equilibrate with environmental moisture during mounting and preparation of the sample for analysis. Hence, changes of the oxygen concentration, measured by ESCA on subsequent samples, were considered unreliable and disregarded.

During the measurement of EBH tagged samples, a decay of the bromine signal with time was observed to occur. Results of measurements on EBH tagged ST-fiber over a 400 minute period are shown in Figure 13 .

The plot is based on "raw data", taking the first count, obtained at a period of time τ as 100%. The time τ for bromine, carbon, and oxygen in this run was 18,27 and 31 minutes, respectively. It will be noted that the correlation for all three elements is composed of two linear segments whose slopes change at the same point in time, i.e., 145 minutes. In the first segment, losses occur in all three elements, while in the second segment only bromine is lost, oxygen stays constant, and carbon increases.

The correlation may be rationalized by assuming for the first segment a first order desorption process of species held by physical forces at the surface. These species might be

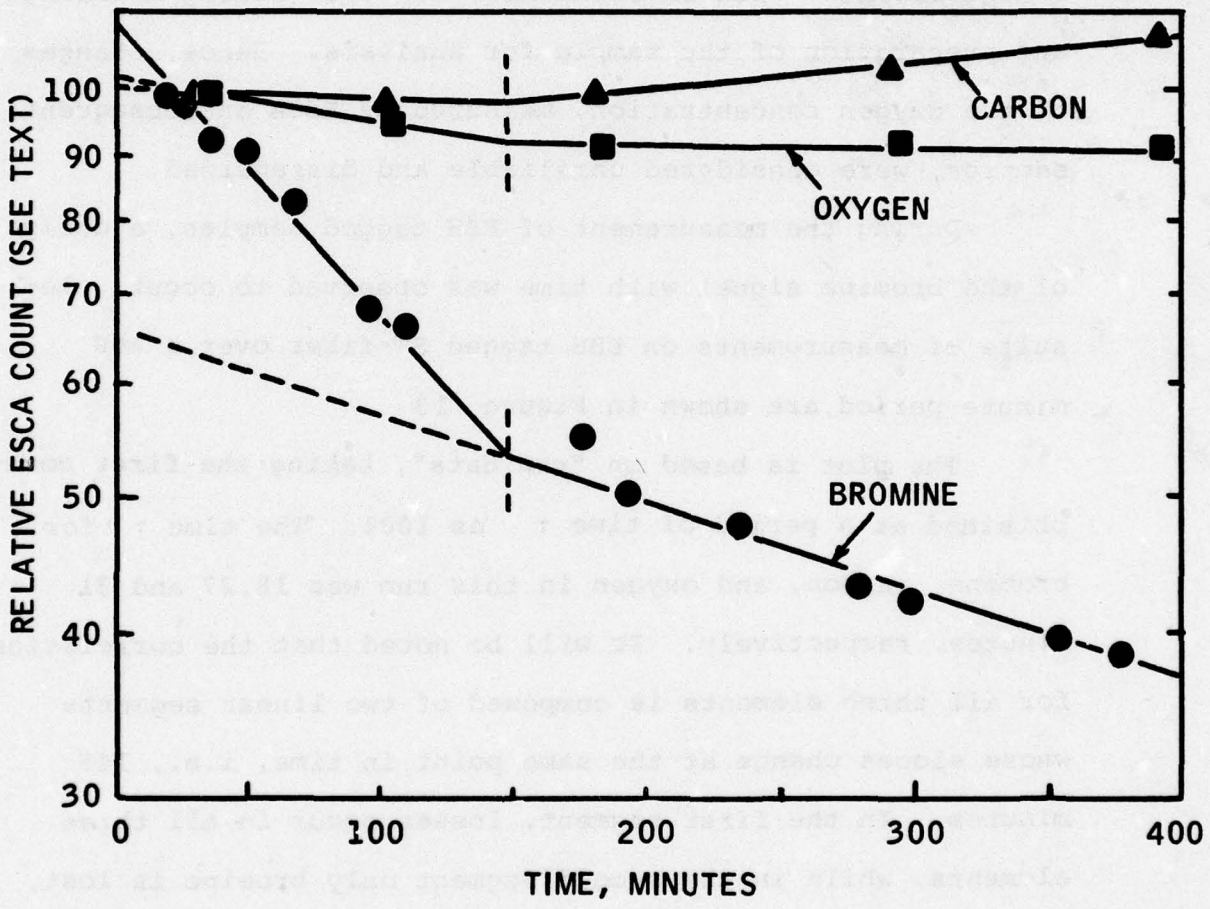

Figure 13. Change of ESCA Species in Epibromohydrin Tagged ST. Fiber

adsorbed epibromohydrin or its corresponding glycol, CO_2, and H_2O, and would lead to losses of Br, C, and O from the substrate. The second segment involves a first order loss of bromine due to X-ray bombardment, without significant losses of oxygen and carbon, i.e., with degradation of the chemisorbed bromine group as the rate controlling step. The loss of bromine would uncover new carbons, and, hence, increase the carbon count.

This interpretation is supported by data presented in Figure 14 which shows the results of ESCA runs on an ST-type and a GR-type fiber, both derivatized with epibromohydrin. Data of Figure 13 have been included, and are identified as ST-2. All points were plotted on a normalized basis, i.e., based on a 100% count at time zero.

With the foregoing assumptions, i.e., the presence of two simultaneous reactions without mutual interference, one may write for the time dependence of the first order decay reaction of bromine

$$- \frac{dX}{dt} = (k_1 + k_2) \quad X$$

where X is the bromine concentration, and k_1 and k_2 are the rate constants for desorption and degradation by bombardment, respectively. Both rate constants would be a function of temperature and pressure in the ESCA instrument, and k_2, in addition, a function of the X-ray intensity. At constant

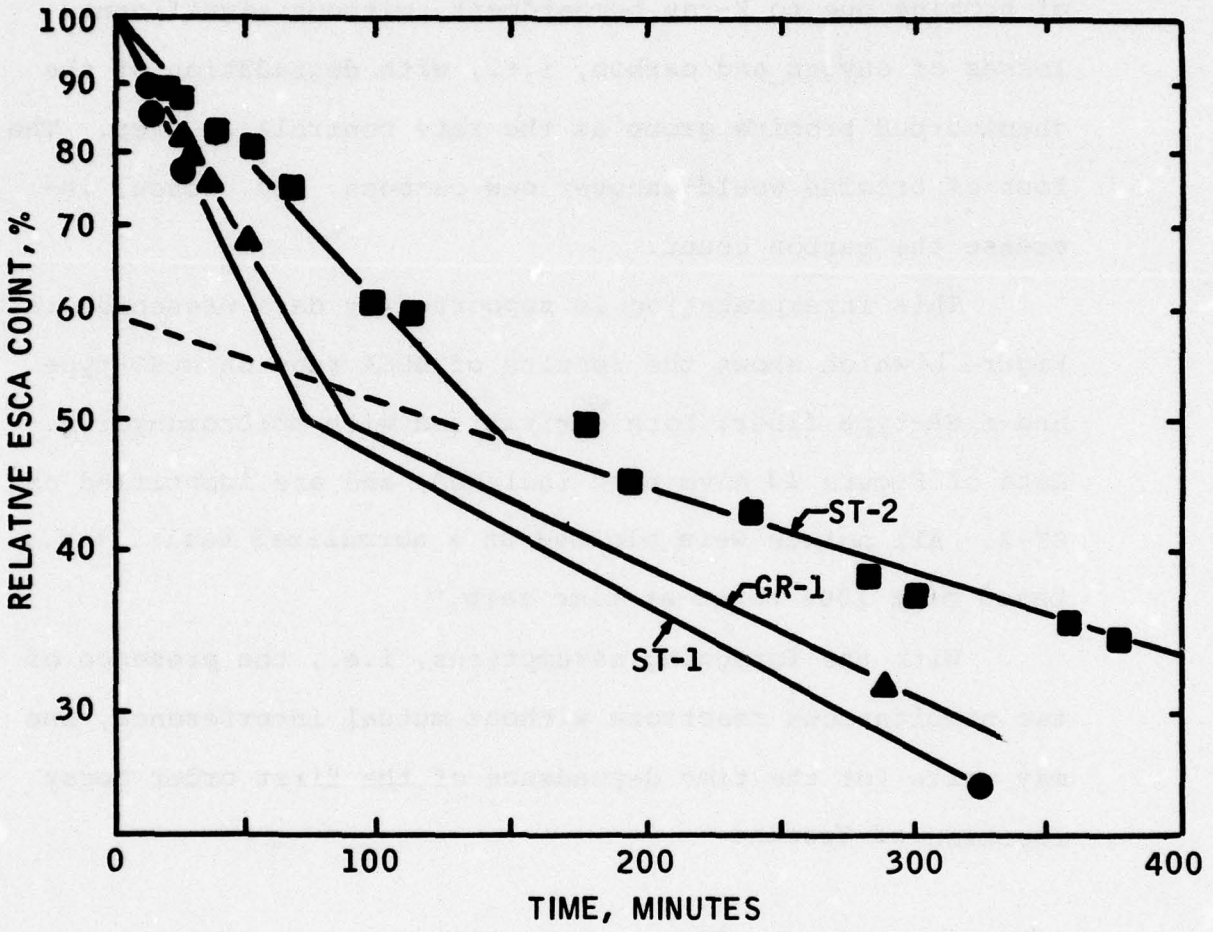

Figure 14. Loss of Bromine in ESCA for Epibromohydrin Tagged Fibers.

X-ray intensity and constant temperature, k_1 and k_2 would depend only on the pressure in the instrument. For this case, the ratio of k_1/k_2 values for all samples would be constant. This is borne out by data listed in Table VII.

TABLE VII

RATE CONSTANTS (min^{-1}) FROM ESCA RUNS OF EPIBROMOHYDRIN TAGGED ST- AND GR-FIBERS

	$10^3(k_1+k_2)$	10^3k_2	10^3k_1	k_1/k_2
ST-1	-9.21	-2.76	-6.45	2.33
ST-2	-4.88	-1.45	-3.43	2.37
GR-1	-7.69	-2.30	-5.38	2.34

Values for $k_1 + k_2$ were obtained from the slope of the initial branch of the correlations, and k_2 from the second branch, assuming complete desorption of the adsorbed species, i.e., $k_1 = 0$. Extrapolations of the second segment of the curve to time zero indicates the ratio of physically adsorbed to chemisorbed bromine species to be 40/60. Based on actual carbon and bromine counts, both corrected for relative intensities, a nominal "surface" concentration of bromine equal to 1.33% in the ST-fiber and 0.55% in the GR-fiber was calculated, of which 60% (relative) are tied to the fiber "surface"

by chemical bonding. Due to the penetration of X-rays into the fiber, the carbon count represents multiple layers of carbon, while the bromine count results from a single layer. Thus, "surface" concentrationsobtained in this manner remain to be corrected for the depth of penetration of the X-rays.

In order to circumvent the uncertainties associated with this procedure, the absolute concentration of bromine, and thereby of reactive surface groups,were obtained via neutron activation analysis which yields the total amount of bromine contained in the sample (see below).

During the work with graphite fibers, a frequent break-down of the ESCA instrument was experienced. An analysis of the cause for this problem suggested that minute fiber fragments lifted off the sample surface and led to sparking in the high-voltage gradient between sample and screen. This problem was found to be inherent in the design of the instrument available for our work which was the first Varian prototype ESCA. Attempts to overcome the break-down by redesigning the sample holder failed due to an extensive reduction of sample surface area and the solid angle of collection.

As an alternate approach, it was decided to continue the investigation with powderized graphite fiber (see Experimental Section), since prior experience had shown that the ESCA instrument would function without break-down with this type of sample configuration. In addition, it was thought advantageous to increase the surface area of the graphite

samples, relative to their weight, in order to gain a higher precision in the subsequent kinetic degradation work. As anticipated, no instrument failures occurred thereafter.

Figure 15 shows results of an ESCA run with EBH tagged ST-powder over an extended time period. Data points for a duplicate scan have been included in the figure and indicate good reproducibility. As observed with EBH tagged fibers, the ESCA time scan yielded again a curve composed of two branches. Extrapolation of the second branch is seen to yield an 85% intercept for chemisorbed species. This improvement was probably due to the more extensive washing and longer drying period used in the preparation of the tagged material. It will be noted that the rate constant for degradation by X-ray bombardment, k_2, is in the same range as had been found for the tagged fiber samples, indicating the presence of the same mechanism of Br-loss. By contrast, the rate constant for desorption of physically adsorbed material was considerably lower than with fibers, suggesting that the material is better retained on the high energy surface produced by milling.

It is also of interest to compare absolute ESCA counts of C, O, and Br from the previously tagged surface treated fiber (identified as ST-2 in Figure 14) with those of the ST-powder samples, in order to gauge the effect of cryo-milling on surface reactivity. Pertinent data are summarized in Table VIII .

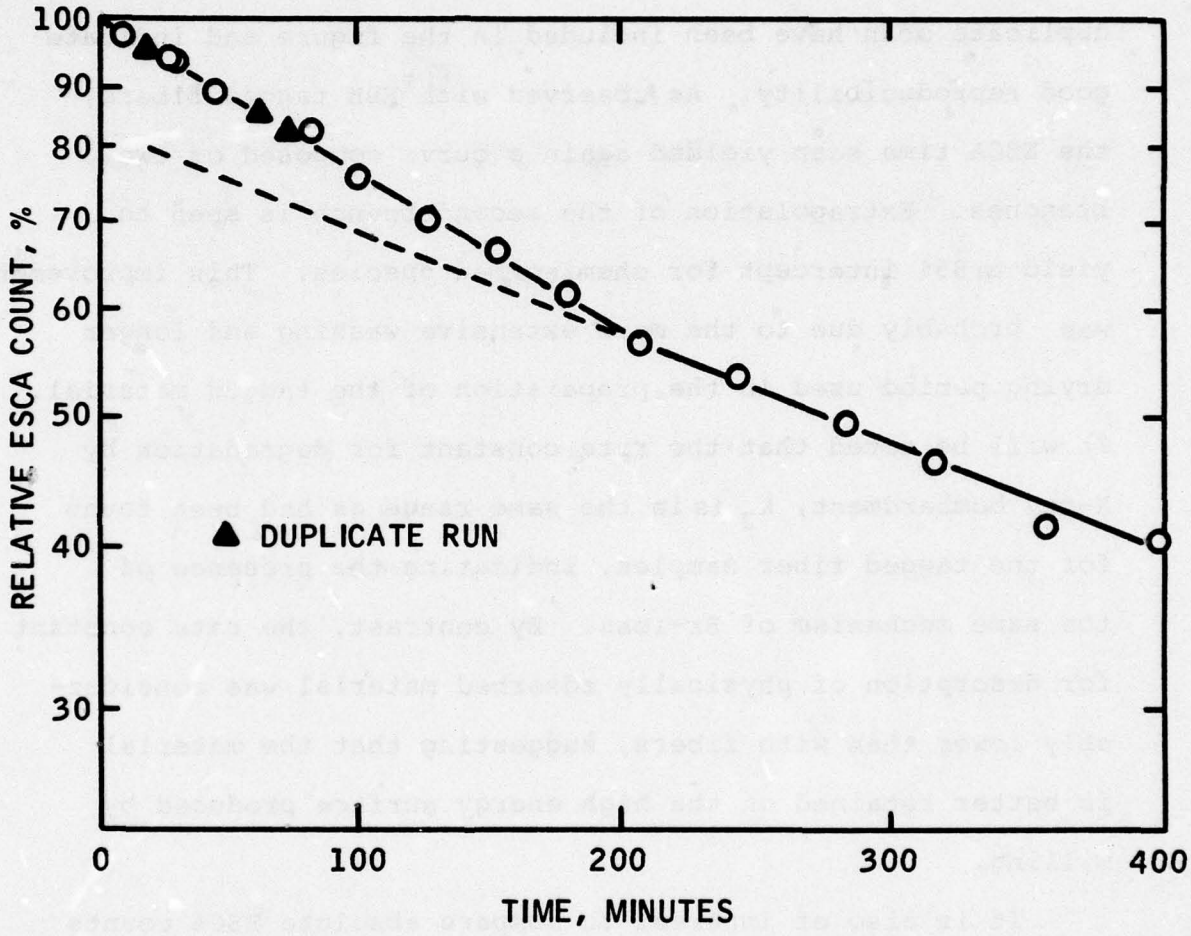

Figure 15. Loss of Bromine in ESCA for Epibromyhydrin Tagged ST-Powder.

TABLE VIII

ABSOLUTE ATOM COUNTS IN ESCA

	ST-2 Fiber		ST-Powder		Ratio of Chemisorbed Elements
	Total	Chemisorbed[1]	Total	Chemisorbed[2]	ST-Fiber/ST-Powder
Br	2000	1200[3]	5900	5000[4]	4.16
C	62000	37200	138500	117700	3.16
O	34000	20400	27300	23200	1.14

(1) 60% chemisorbed

(2) 85% chemisorbed

(3) bromine count 3.2% in respect to carbon count.

(4) bromine count 4.2% in respect to carbon count.

The comparison shows that the absolute counts of chemisorbed C and Br have been increased by cryo-milling by about the same ratio, implying also that the C/Br ratio has been maintained at a comparable level. By contrast, the oxygen count has remained almost constant. While the carbon count increase indicates that the surface coverage of the sample in the ESCA holder had been increased due to milling and better packing, it appears that the surface oxidation of the milled material had yielded about the same surface and had not led to the additional formation of non-taggable sites.

In order to determine hydroxyl type surface groups, ST-powder was tagged with 3,5-dinitrobenzoyl chloride, a reagent

which is specific for phenols, yielding the corresponding 3,5-dinitrobenzoic ester without reacting with carboxyl groups. The nitrogen content of the tagged material was measured by ESCA. It was found to be 0.35%, based on carbon count. With two nitrogen atoms per site tagged, the phenolic OH concentration on the graphite powder surface would be 0.17% based on carbon count. Due to the weak ESCA signal, this concentration must be considered a crude estimate, with a probable precision of ± 20% relative. It indicates, however, that compared to the total concentration of epoxidizable groups of 4.2 %, based on carbon count (Table VIII), the concentration of phenolic hydroxyl group at the surface of the ST-powder is low. Assuming that the total epoxidizable groups are composed of carboxyl and hydroxyl groups, the distribution would be 96/4, respectively.

This low concentration of phenolic type surface sites suggests that degradation of epoxidizable groups at the fiber/resin matrix interface would be primarily due to cleavage of the remaining ester bonds from carboxyl group surface sites. Since ester bonds are more sensitive to cleavage in an uncatalized environment than ether bonds, the degradation kinetics of epoxidized surface sites was expected to adhere to a classical first order ester hydrolysis reaction.

2. DEGRADATION OF TAGGED SURFACE SITES

The objective of this work phase was to determine the

rates of disappearance of tagged groups as a function of temperature under wet (100% R_H) and dry conditions, with the purpose of comparing them with the rates of strength loss observed in composites under the same conditions. The bromine atom of the EBH tagged surface sites was used as an indicator and its loss followed by ESCA measurements. The experimental technique has been described in the Experimental Section.

In the evaluation of ESCA data it was observed that the thermal treatment of the samples in the degradation environment yielded material which contained varying amounts of physically adsorbed bromine species. This occurred although the work-up procedure after the degradation experiment had been standardized. These differences are illustrated in Figure 16 which shows the time decay curves of the ESCA count for EBH tagged ST-powder after hydrolysis at 150°C for 2 and 4 hours. It will be noted that the sample exposed for 2 hours indicates a level of 95% of the bromine present as chemisorbed species, while the 4-hours sample indicates only 78%.

This variation necessitated the determination of the actual amount of chemisorbed species for each sample generated in the degradation experiments. From this data a chemisorbed bromine count was obtained which could be used to calculate the amount of chemisorbed species lost by the environmental treatment. Table IX exemplifies this evaluation scheme for

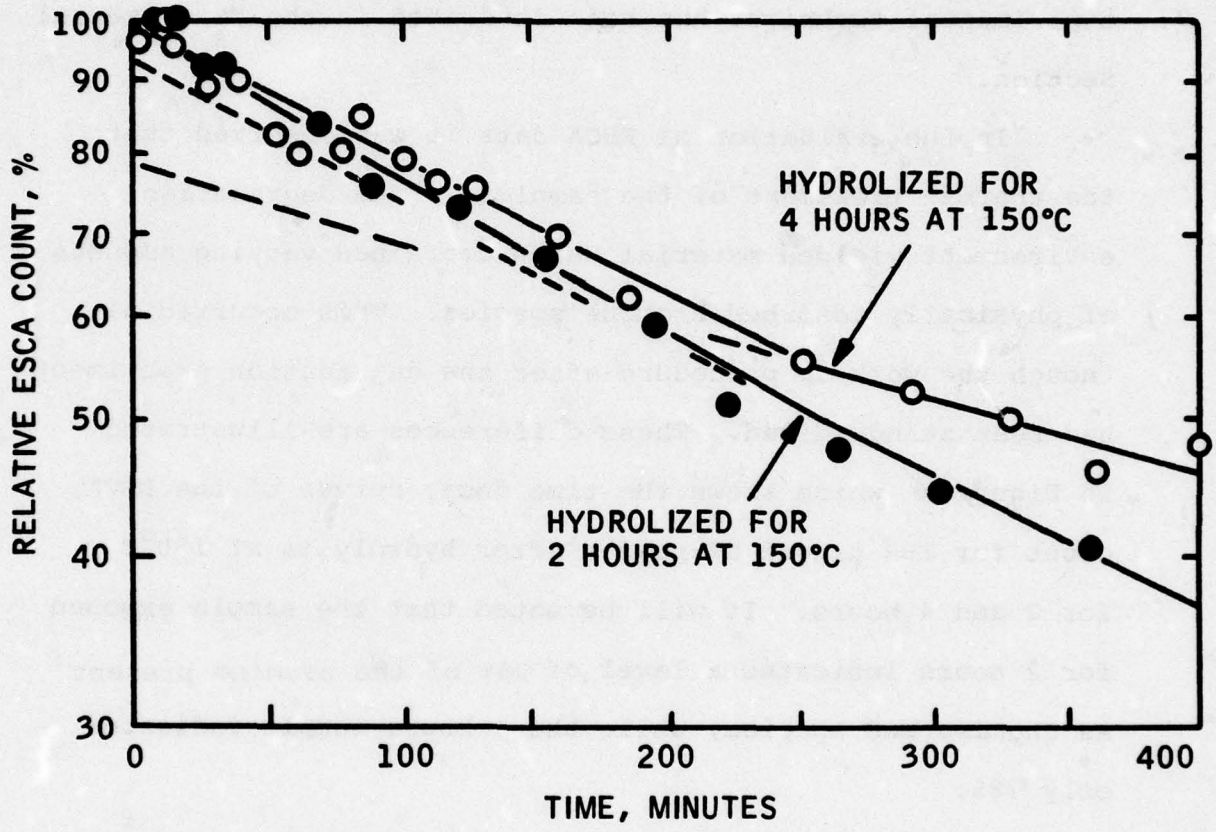

Figure 16. Loss of Bromine in ESCA for Hydrolyzed Epibromohydrin Tagged ST-Powder.

data of EBH tagged ST-powder hyrolized at 150°C. It will be noted that the raw ESCA counts for carbon also vary due to variations in the packing density of the samples in the sample holder. Thus, the raw ESCA counts for bromine had to be normalized to the raw carbon count of the control. The normalized raw bromine counts thus obtained were then converted to the chemisorbed bromine count, knowing the percent of chemisorbed species from the ESCA time decay curve.

TABLE IX

EVALUATION OF KINETIC ESCA DATA

(EBH tagged ST-Powder, 150°C, 100% R_H)

Reaction Time Hours	ESCA Counts Br/C	Normal-ized Br Count	Chemi-sorbed Br (%)	Chemi-sorbed Br count	Retained Br (%)
Control	5705/139237	5705	88	5000	100.0
2	2182/113398	2679	95	2545	50.9
3	1582/116328	1894	95	1800	36.0
4	1387/117660	1641	78	1280	25.6

Based on this evaluation scheme, data for the hydrolysis of EBH tagged ST-powder in the temperature range of 100 to

150°C have been compiled in Table X . These are plotted in Figure 17 for a first order reaction in respect to bromine assuming the conventional rate relationship $-dX = k_h X\, dt$, where X represents the bromine concentration, and k_h the rate constant for hydrolysis which may be assumed to be a function of the relative humidity in the environment (see below).

TABLE X

HYDROLYSIS OF EPI BROMOHYDRIN TAGGED ST-POWDER AT 100% RELATIVE HUMIDITY

Temperature (°C)	Bromine Retained (%) 1 hr.	2hrs.	3 hrs.	4 hrs.	Rate Constant for Hydrolysis (hr^{-1})
100	98.2	92.1		89.4	0.028_1
125	85.5	81.7		66.1	0.105
135	81.0	67.5		48.2	0.18_5
150		50.9	36.0	25.6	0.34_0

Experiments to determine the rate of thermal degradation of interface bonds were carried out with the same master batch of EBH tagged ST-powder in the same glass tubes as the hydrolysis

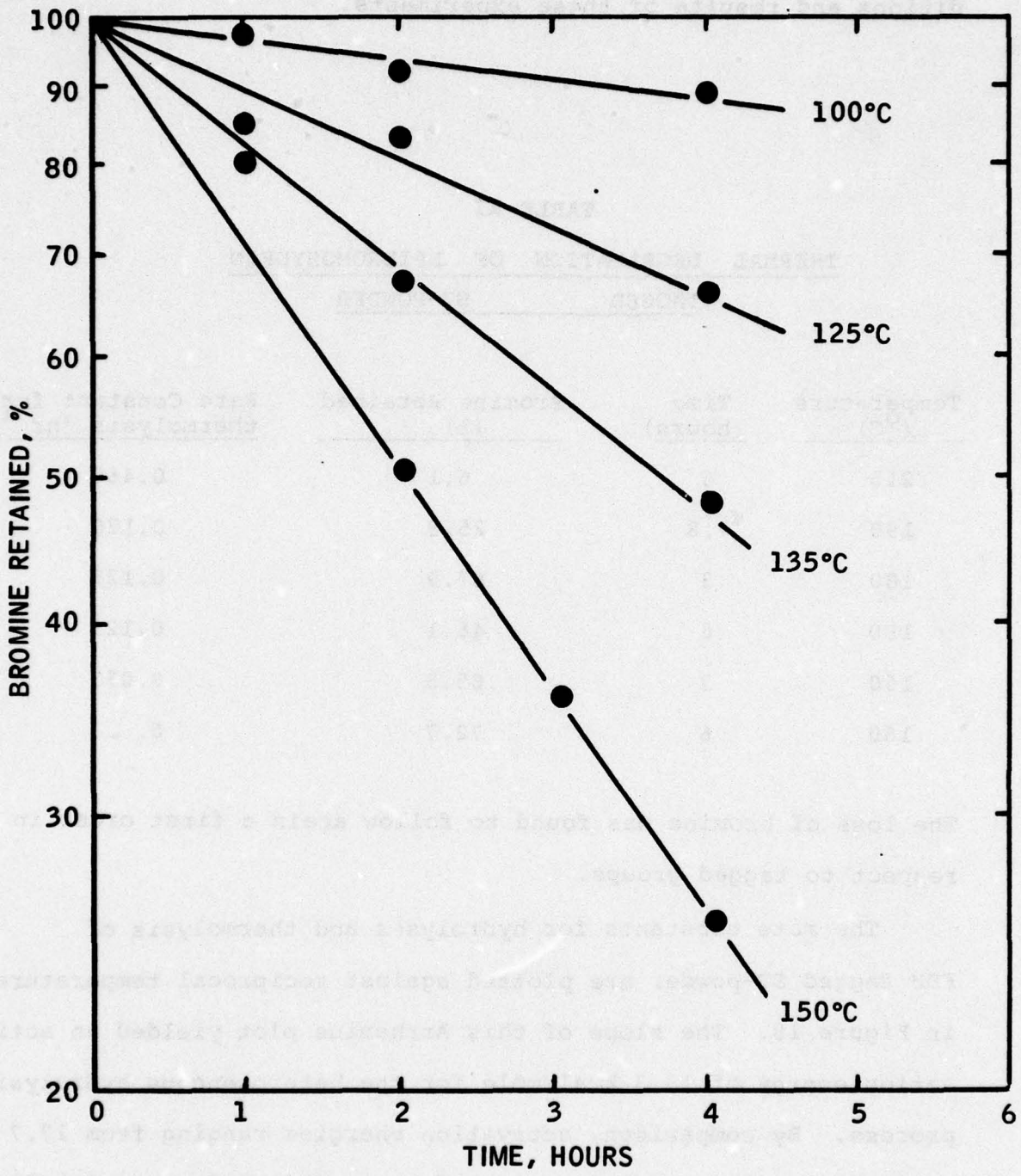

Figure 17. Amount of Bromine Retained in Epibromohydrin Tagged ST-Powder after Hydrolysis at Various Temperatures.
(First Order Plot)

experiments, but in the absence of water. Table XI lists conditions and results of these experiments.

TABLE XI

THERMAL DEGRADATION OF EPIBROMOHYDRIN TAGGED ST-POWDER

Temperature (°C)	Time (hours)	Bromine Retained (%)	Rate Constant for thermolysis (hr^{-1})
215	6	6.1	0.466
190	7.8	25.8	0.170
180	3	67.9	0.129
180	6	46.1	0.129
160	3	85.3	0.053
160	6	72.7	0.053

The loss of bromine was found to follow again a first order in respect to tagged groups.

The rate constants for hydrolysis and thermolysis of EBH tagged ST-powder are plotted against reciprocal temperature in Figure 18. The slope of this Arrhenius plot yielded an activation energy of 16.3 kcal/mole for the heterogeneous hydrolysis process. By comparison, activation energies ranging from 17.7 to 20 kcal/mole have been reported by Ingold (Reference 32) for the hydrolysis of p-substituted benzoic acids in an homogeneous medium. They are very sensitive to the type and degree of

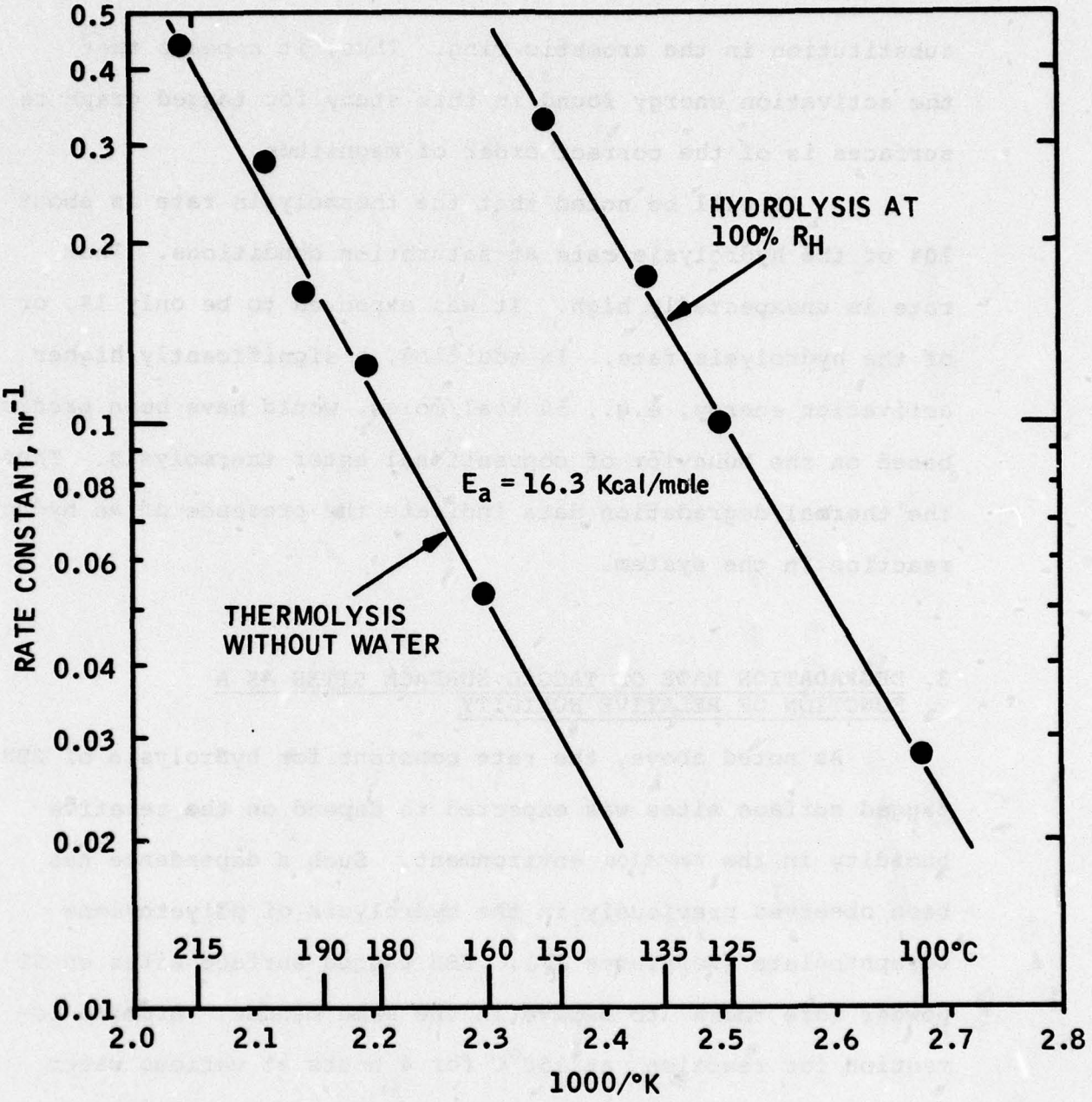

Figure 18. Arrhenius Plot for Hydrolytic and Thermal degradation of Epibromohydrin Tagged S1-Powder.

substitution in the aromatic ring. Thus, it appears that the activation energy found in this study for tagged graphite surfaces is of the correct order of magnitude.

It will be noted that the thermolysis rate is about 10% of the hydrolysis rate at saturation conditions. That rate is unexpectedly high. It was expected to be only 1%, or less, of the hydrolysis rate. In addition, a significantly higher activation energy, e.g., 50 kcal/moles, would have been predicted based on the behavior of conventional ester thermolysis. Thus, the thermal degradation data indicate the presence of an hydrolysis reaction in the system.

3. DEGRADATION RATE OF TAGGED SURFACE SITES AS A FUNCTION OF RELATIVE HUMIDITY

As noted above, the rate constant for hydrolysis of EBH tagged surface sites was expected to depend on the relative humidity in the reaction environment. Such a dependence has been observed previously in the hydrolysis of polyethylene terephthalate (Reference 33). EBH tagged surface sites on ST-powder were found to behave in the same manner. Bromine retention for reaction at 150°C for 4 hours at various water levels in the reaction tube are summarized in Table XII and plotted in Figure 19. The correlation is linear with an intercept of 90.0% retained bromine at zero water added to the tube. From the thermolysis kinetics, a value of 88.7% retained

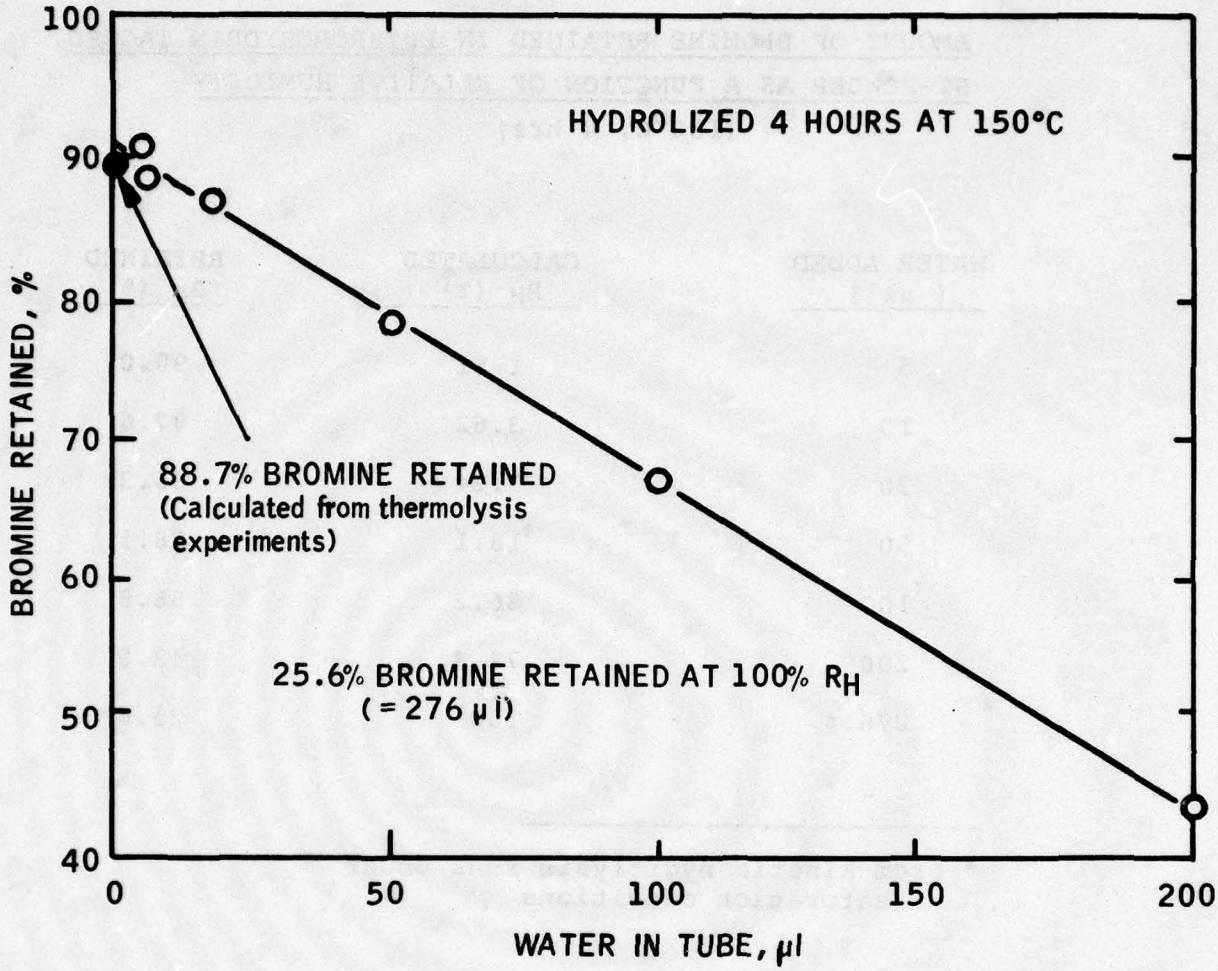

Figure 19. Amount of Bromine Retained in Epibromohydrin Tagged St-Powder after Hydrolysis at Various Water Levels.

TABLE XII

AMOUNT OF BROMINE RETAINED IN EPIBROMOHYDRIN TAGGED ST-POWDER AS A FUNCTION OF RELATIVE HUMIDITY

(150°C, 4 hrs)

WATER ADDED (µℓ)	CALCULATED R_H (%)	RETAINED Br (%)
5	1.81	90.0
10	3.62	87.6
20	7.24	86.3
50	18.1	78.1
100	36.2	66.8
200	72.4	42.9
276.4	100	25.6*

* from kinetic hydrolysis runs under saturation conditions

bromine may be calculated. These two values are within the limits of experimental error of the method, indicating that thermolysis experiments were carried out in the presence of extraneous moisture sources. Hence, it may be concluded that the low activation energy observed in the thermolysis reaction is caused by a moisture source intrinsic in the system. A possible source of this nature might be the pendant hydroxyl group on the epoxy moiety which is formed on reaction between the epoxy group and the functional group at the graphite surface. This pendant hydroxyl group could cleave the ester bond in a concerted mechanism even at water-free conditions in the environment. In the presence of additional water, as in a humid environment, this reaction would obviously be accelerated proportional to the moisture level available to the interface. If so, this reaction path would be an intrinsic property of graphite/epoxy resin composites and would not be eliminated by cladding with a moisture impervious metal film, as has been suggested (Reference [5]).

The relative humidity in these experiments may be estimated from the definition of relative humidity, $R_H = 100p'_w / p^o_w$, where p'_w is the partial pressure of water in the reaction volume, and p^o_w is the saturation pressure at 150°C (=3570.48 mm Hg, from steam tables). The partial pressure of water, p'_w, as a function of the amount of water $[\mu\ell]$ added to the tube volume $\left[V_T = 0.083\ \ell\right]$ may be obtained by assuming ideal gas

behavior for the molar volume of water vapor $\left[V_W = 22.4\ell/18\ gm\right]$. Thus, for 150°C

$$p'_w = \frac{V_W}{V_T} \cdot \frac{T_1}{T_2} \quad 760$$

$$= \frac{10^{-3}(gm/\mu\ell)}{18(gm/M)} \cdot \frac{22.4(\ell/M)}{0.083\ (\ell)} \cdot \frac{423(^oK)}{373(^oK)}\ 760(mmHg)$$

$$= 12.92\ (mm\ Hg/\mu\ell)$$

Resubstitution of this value for p'_w into the definition equation yields $R_H = 0.362\ (\%/\mu\ell)$ i.e. for 100% R_H in this reaction volume, the addition of 276.4 $\mu\ell$ of water is required.

4. NEUTRON ACTIVATION ANALYSIS RESULTS

Hydrolized and thermolized samples of EBH tagged ST-fiber and ST-powder were subjected to neutron activation analysis (NAA). In contrast to the relative bromine counts produced by ESCA, NAA yields direct concentrations of the analyzed species in ppm. Thus, the purpose of obtaining NAA data on the degraded samples was two-fold: to compare the behavior of powder and fiber in respect to their reactivity under hydrolysis conditions, and to provide absolute concentrations of tagged sites in the substrate which then could be converted to surface site concentrations, via surface area data determined separately.

NAA data are compiled in Table XIII and plotted according to the conventional Arrhenius relationship in Figure 20 , ESCA data have been included in Figure 20.

Data in Table XIII were obtained from raw NAA results by applying the same corrections for the respective amounts of chemisorbed bromine species as has been done with ESCA data.

It is obvious that both type of data show good agreement, indicating that ESCA and NAA yield corresponding results. It is also seen that powder and fiber data are essentially the same, confirming that the reactivity of surface sites on powder and fiber were identical.

5. CONCENTRATION OF EPOXIDIZABLE SURFACE SITES

NAA data may be used to estimate the concentration of epoxidizable surface groups on ST-fiber and ST-powder. The estimate is obtained by converting the weight bulk concentrations (ppm) into molar bulk concentrations (μM Br/gm substrate), using 79.9 as the molecular weight of bromine. Assuming that all of the bromine is contained at the surface, and that one site covers the area of a single carbon atom ($10^{-20} m^2$), the total surface area occupied by the sites is calculated, using the Avogadro Number of 6.02×10^{23} molecules/mole. Pertinent data are summarized in Table XIV . The surface coverage of

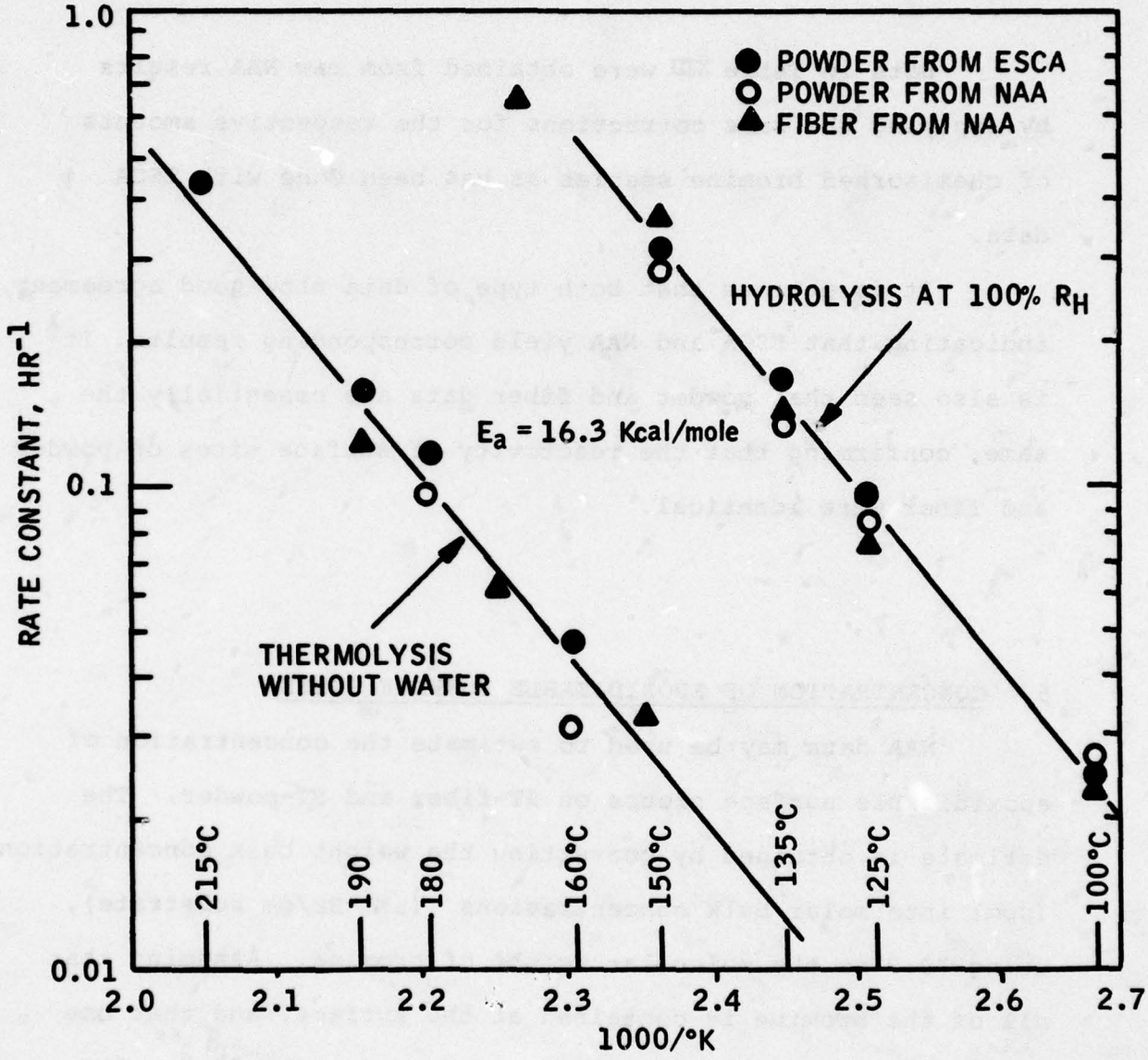

Figure 20. Arrhenius Plot for Hydrolytic and Thermal Degradation of Epibromohydrin Tagged ST-Powder and ST-Fiber.

TABLE XIII

COMPARISON OF RATE CONSTANTS FOR HYDROLIZED AND THERMOLIZED EPIBROMOHYDRIN TAGGED POWDER AND FIBER, OBTAIND BY NAA

	Reaction (°C)	Time (hr.)	NAA-bromine Powder (ppm)	NAA-bromine Fiber (ppm)	Rate Constant (hr^{-1}) Powder	Rate Constant (hr^{-1}) Fiber
Hydrolysis	100	0	6400	126		
		1	6260	123		
		2	--	122		
		4	5630	114	0.029	0.026
	125	0	6400	100		
		1	5670	93		
		2	5340	85		
		4	4400	73	0.094	0.082
	135	0	6400	100		
		1	5500	83		
		2	4780	76		
		4	--	55	0.148	0.149
	150	0	6400	148		
		1	4460	--		
		2	3210	--		
		4	1835	30	0.335	0.400
	170	0		148		
		4		11		
		5		6	--	0.640
Thermolysis	150	0		140		
		4		130		
		5		125		
		7		116		0.037
	160	0	6600			
		3	6010			
		6	5370		0.034	
	170	0		148		
		4		110		
		5		105		
		7		93		0.066
	180	0	6600			
		3	4850			
		6	3510		0.016	
	190	0 5	6600	148		
		6 7	2940	84	0.135	0.115

TABLE XIV

CONCENTRATIONS OF EPOXIDIZABLE SURFACE SITES ON ST-FIBER AND POWDER

	ST-FIBER	POWDER
NAA-Bromine (ppm)	185	7530
Hydrolizable Bromine (ppm)	148	6400
Hydrolizable Bromine (%)	80	85
Hydrolizable Bromine (μM/gm)	1.85	80
Surface Area Occupied by tagged sites[1] (m^2/gm)	0.011	0.48
Total Surface Area from Adsorption Measurements (m^2/gm)	0.740	24.0
Coverage of epoxidizable Surface Groups (%)	1.51	2.0
Hydroxyl/carboxyl Group ratio	-	4/96

[1] Based on an area of 10^{-20} (m^2) occupied by one carbon atom on a tagged site

active sites, shown in the Table, is based on values for the total available surface area determined by the BET method (Table V).

It is seen that the portion of the ST-fiber surface covered by epoxidizable groups is only 1.5%, and for the ST-powder is 2.0%. The somewhat higher value for the ST-powder may be rationalized by the relatively more severe oxidation conditions empolyed in its preparation.

Similar effects have been observed on other carbon based fibers. Thus, a 1.2% coverage has been reported (Reference 10) for Thornel 25 ($1m^2/gm$ available surface) and 2% for nitric acid oxidized Thornel 25 ($12m^2/gm$). These data were obtained by using a titration method. Likewise, a 2.6% coverage has been found on highly graphitized carbon black (Reference 16) by an oxygen chemisorption method.

6. DEGRADATION OF GRAPHITE FIBER/EPOXY RESIN COMPOSITES

The objective of this segment of work was to correlate hydrolytic and thermolytic degradation data, obtained on epibromohydrin tagged fibers, with the deterioration of physical properties of graphite fiber/epoxy resin composites. The physical property chosen as a gauge for composite degradation was interlaminar shear which is generally thought to reflect most closely changes of the fiber/resin interface, and, hence, should be associated with the degradation chemistry in this region. In

addition, flexural strength was to be determined. Any correlation between surface group degradation from tagged fiber and composite degradation was to be based on a comparison of rates and activation energies, whereby the elucidation of irreversible processes was to be of prime importance.

Degradation experiments with graphite fiber/epoxy resin composites were carried out in a dry and a wet (submerged in water) environment, at temperatures ranging from 85°C to 210°C, and for reaction times from one to ten days. The response of short beam (4:1) shear strength, flexural (32:1) strength and flexural modulus to the various reaction conditions was determined. Data obtained are listed in Tables XV and XVIII.

Short beam shear strengths in Table XV are given in PSI and in per cent of short beam shear strength retained against the control. All 3 and 10 day samples collected from wet conditions were dried in vacuo at 85°C to a common moisture level of 0.3 $\pm$ 0.05%. Samples collected after one and two days hydrolysis were tested "as is" at the moisture levels listed, or dried in vacuo at 85°C as the other samples. Samples resulting from dry degradation conditions (thermolysis) were tested dry, i.e.at a moisture level of zero. Further drying of these samples at 85°C in vacuo for up to 3 days yielded no change in short beam shear strength. Degradation experiments (not listed in Table XV) were also carried out at 85°C for up to 10 days, but indicated no degradation of short beam shear strength.

From data of Table XV it is apparent that the magnitude of decay of short beam shear strength depends on the moisture

TABLE XV

SHORT BEAM SHEAR STRENGTH DATA FOR THERMALLY TREATED COMPOSITE SAMPLES (PSI)*

TEMPERATURE OF EXPOSURE	CONTROL	Time of Exposure (Days) 1	2	3	10
		WET CONDITIONS (100% R_H)			
150°C	8890			8350 (93.9%)	7460 (83.9%)
190°C	8560			7540 (88.1%)	6850 (80.0%)
	9120	8460[1] (92.7%)	8000[2] (87.7%)		
		8680 (95.1%)	8200 (90.0%)		
210°C	8250	6920[3] (83.9%)	6590[4] (79.8%)	6900 (83.7%)	6160 (74.7%)
	7620 (93.3%)	7300 (88.5%)			
		DRY CONDITIONS			
150°C	8890			8890 (100%)	8960 (100.8%)
190°C	9120			8560 (93.6%)	8370 (91.7%)
210°C	8250			7680 (93.1%)	7150 (86.7%)

*Average values from 6 specimen; standard deviations were ± 2%; All samples showed shear failure.

[1] Tested at 1.4 wt.% moisture level

[2] Tested at 1.6 wt.% moisture level

[3] Tested at 2.2 wt.% moisture level

[4] Tested at 2.6 wt.% moisture level

All other samples dried to 0.3 wt.% moisture level (85°C, 2 days, 300mm Hg).

content of the specimen at testing. As indicated by the one and two day data, a portion of the decay is recoverable on drying at 85°C in vacuo to the 0.3% moisture level. The amount recovered depends apparently on the moisture content of the specimen, i.e., it is higher with higher moisture content. Additional drying below the 0.3% moisture level showed no further changes in the short beam shear strength. Thus, the remaining data shown in Table XV represent the irreversible portion of the short beam shear strength decay. Within the time frame of these experiments, the decay under dry conditions becomes measurable only above 150°C, and reaches at 210°C the level equivalent to the decay under wet conditions at 150°C. It is obvious that interlaminar shear strength loss is accelerated by moisture.

A semilogarithmic (first-order) plot of these data shows that the decay is non-linear with time, in contrast to the linear relationship observed previously with the loss of tagged surface groups from graphite fiber. As seen in Figure 21, the decay rate diminishes with time and appears to approach a constant level. The initial decay rate may be estimated from the tangents of the decay curves at time zero. Table XVI lists the calculated constants for these initial decay rates. The constants are lower than the constants for the degradation of tagged surface groups by some two orders of magnitudes.

An Arrhenius plot (Figure 22) of the initial decay rate constants yields the same slope for wet and dry conditions with

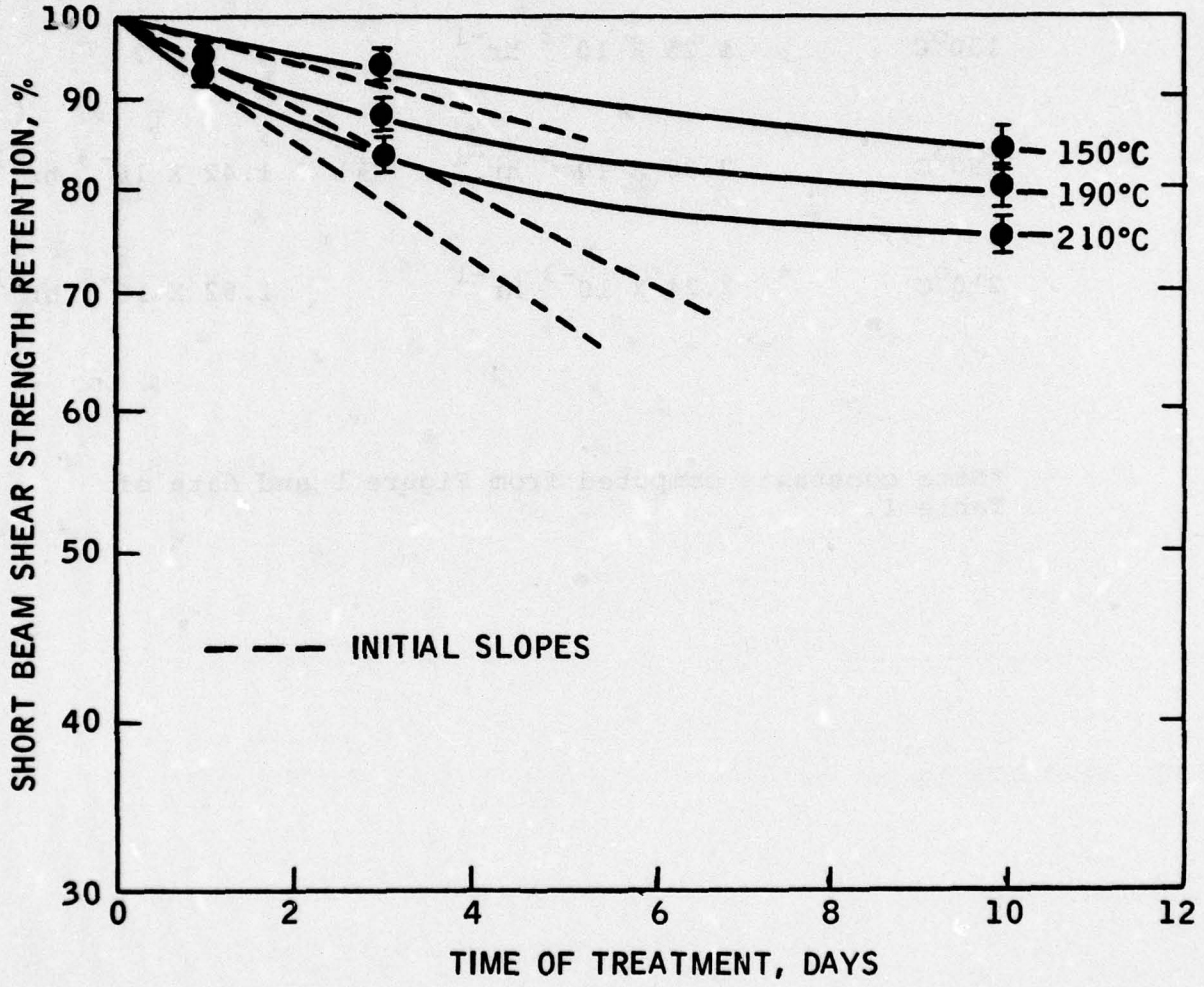

Figure 21. Short Beam Shear Strength Retention of Graphite Fiber/Epoxy Resin Composite with Time of Exposure to a 100% RH Environment.

TABLE XVI

INITIAL DECAY RATES OF SHORT BEAM SHEAR STRENGTHS FOR THERMALLY TREATED COMPOSITE SAMPLES*

	WET	DRY
150°C	1.25×10^{-3} hr^{-1}	?
190°C	2.38×10^{-3} hr^{-1}	1.42×10^{-3} hr^{-1}
210°C	3.24×10^{-3} hr^{-1}	1.92×10^{-3} hr^{-1}

*Rate constants computed from Figure 1 and data of Table I.

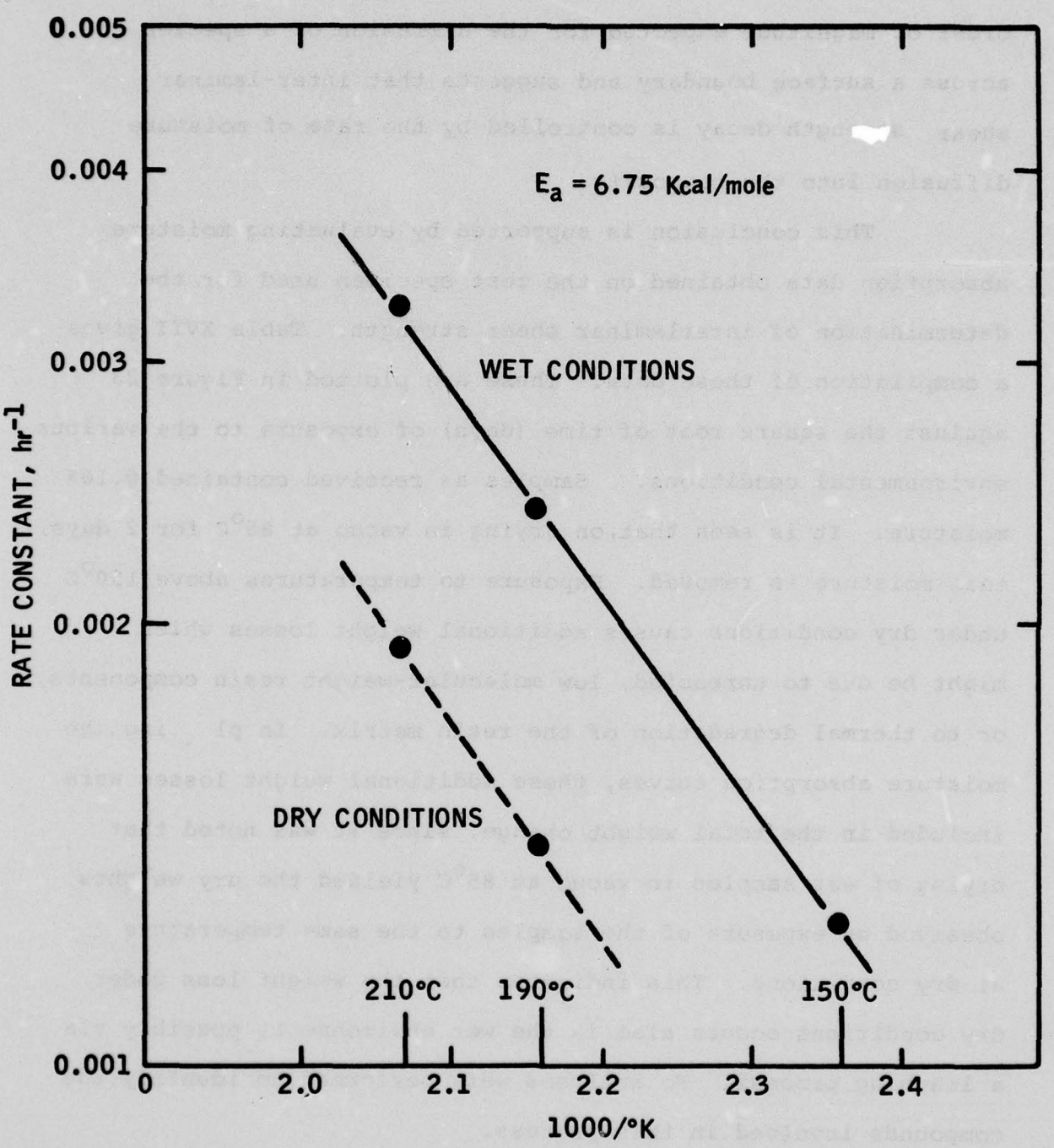

Figure 22. Arrhenius Plot of Initial Decay Rates of Short Beam Shear Strength of Thermally Treated Composite Samples. (Rate Constants from Initial Slopes of Figure 21).

an activation energy of 6.6 Kcal/mole. This value is in the order of magnitude expected for the diffusion of a species across a surface boundary and suggests that inter-laminar shear strength decay is controlled by the rate of moisture diffusion into the composite.

This conclusion is supported by evaluating moisture absorption data obtained on the test specimen used for the determination of interlaminar shear strength. Table XVII gives a compilation of these data. These are plotted in Figure 23 against the square root of time (days) of exposure to the various environmental conditions. Samples as received contained 0.16% moisture. It is seen that, on drying in vacuo at 85°C for 2 days, this moisture is removed. Exposure to temperatures above 150°C under dry conditions causes additional weight losses which might be due to unreacted, low molecular-weight resin components, or to thermal degradation of the resin matrix. In plotting the moisture absorption curves, these additional weight losses were included in the total weight change, since it was noted that drying of wet samples in vacuo at 85°C yielded the dry weights observed on exposure of the samples to the same temperature at dry conditions. This indicates that the weight loss under dry conditions occurs also in the wet environment, possibly via a leaching process. No analyses were performed to identify the compounds involved in this process.

The initial rates of moisture absorption are combined in an Arrhenius plot, shown in Figure 24. The slope of the line indicates an activation energy of 6.7 Kcal/mole for the

TABLE XVII

WEIGHT CHANGES (IN PERCENT OF CONTROL) OF COMPOSITE SAMPLES ON EXPOSURE TO VARIOUS TEMPERATURES AND ENVIRONMENTAL CONDITIONS

TEMPERATURE OF EXPOSURE	ENVIRONMENTAL CONDITION	TIME OF EXPOSURE (DAYS) 1	2	3	4.75	10
85°C	Wet	0.06	0.21		0.42	
	Dry	-0.13	-0.16		-0.16	
	Total Weight Change	0.22	0.37		0.58	
150°C	Wet	0.58	0.82	1.0	1.16	
	Dry	-0.16	-0.16		-0.18	
	Total Weight Change	0.74	0.98	1.17	1.34	
190°C	Wet	1.16	1.36	1.60		1.93
	Dry	-0.22	-0.25	-0.28		-0.38
	Total Weight Change	1.38	1.61	1.88		2.31
210°C	Wet	1.78		2.04		1.81
	Dry	-0.41		-0.59		-0.90
	Total Weight Change	2.19		2.63		2.71

AD-A054 460 CELANESE RESEARCH CO SUMMIT N J F/G 11/2
EFFECTS OF MOISTURE ON CHEMICAL INTERACTIONS AT A POLYMER-FIBER--ETC(U)
DEC 77 D E STUETZ, R E SULLIVAN, A DIEDWARDO F33615-76-C-5223
UNCLASSIFIED AFML-TR-77-214 NL

2 OF 2
AD
A054460

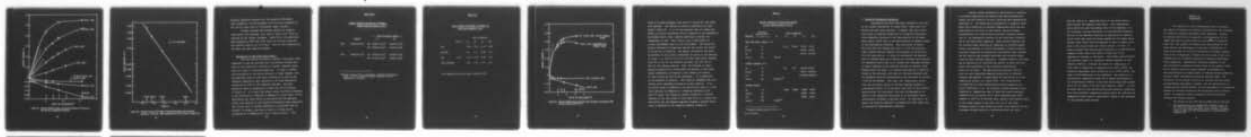

END
DATE
FILMED
6-78
DDC

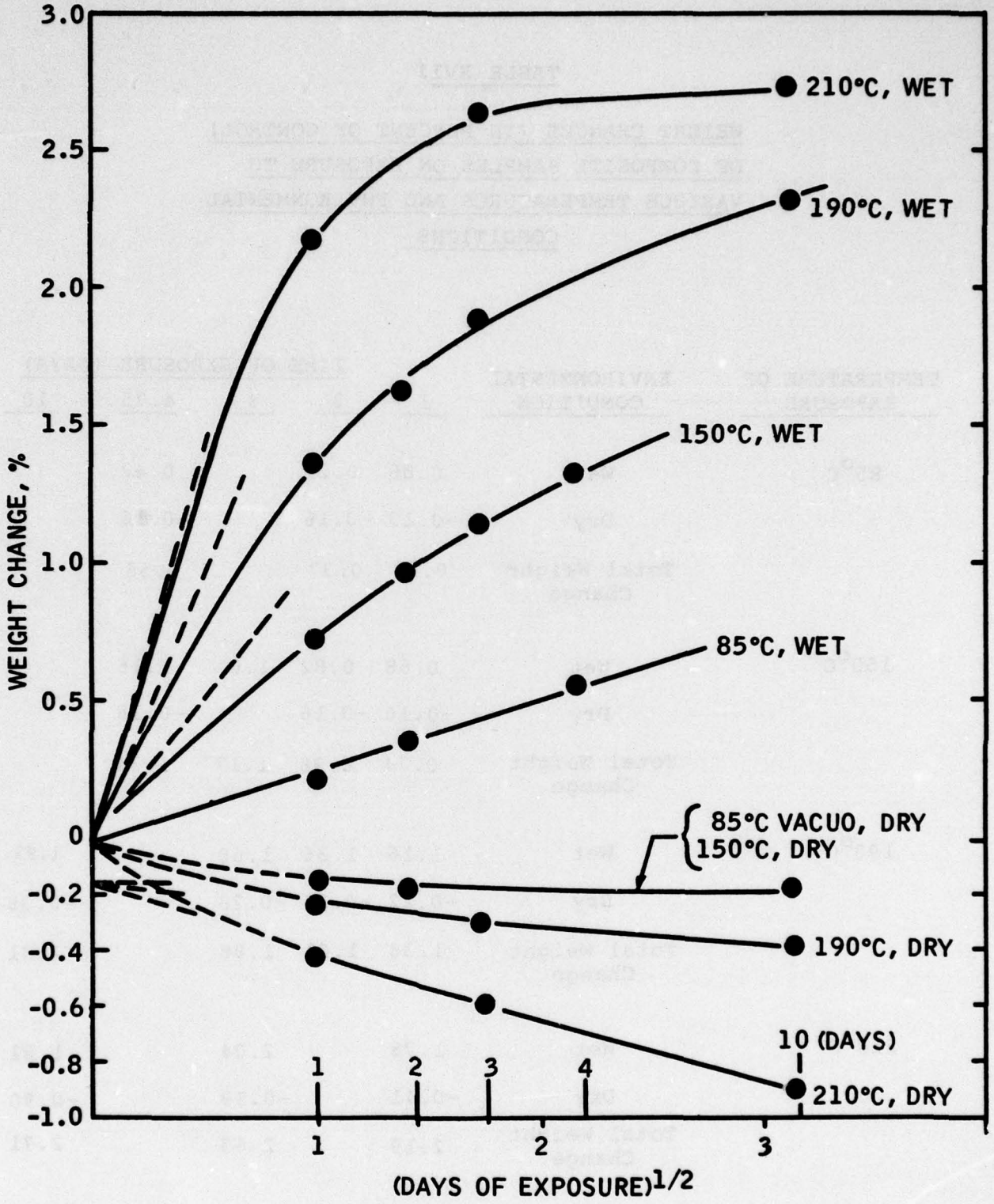

Figure 23. Relative Weight Change of Composite Samples on Exposure to Wet and Dry Temperature Conditions.

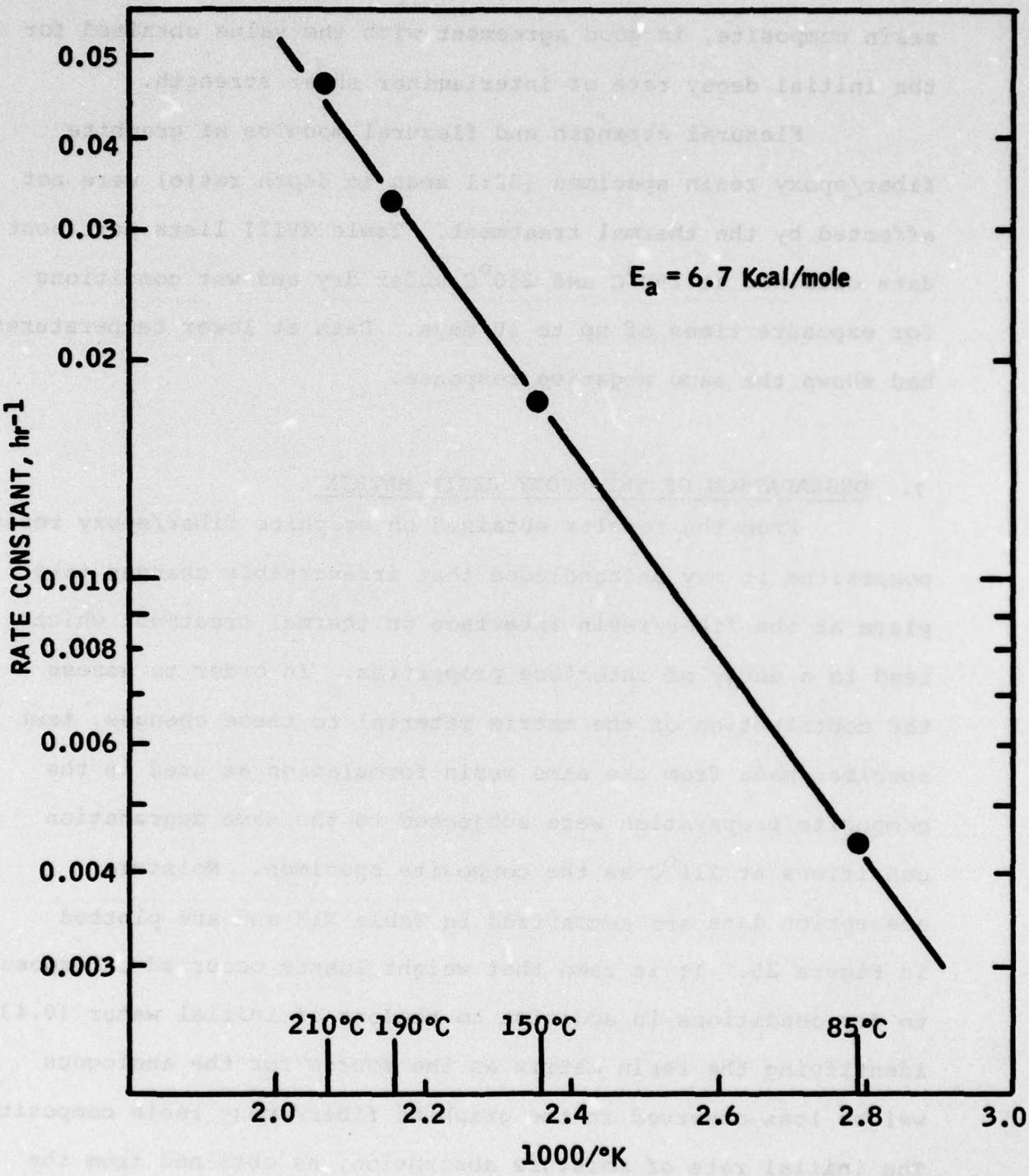

Figure 24. Arrhenius Plot of Initial Rate of Mositure Absorption into Composite Samples at 100% R_H. (Rate Constants from Initial Slopes of Figure 23).

moisture absorption process into the graphite fiber/epoxy resin composite, in good agreement with the value obtained for the initial decay rate of interlaminar shear strength.

Flexural strength and flexural modulus of graphite fiber/epoxy resin specimen (32:1 span to depth ratio) were not affected by the thermal treatment. Table XVIII lists pertinent data obtained at 190°C and 210°C under dry and wet conditions for exposure times of up to 10 days. Data at lower temperatures had shown the same negative response.

7. DEGRADATION OF THE EPOXY RESIN MATRIX

From the results obtained on graphite fiber/epoxy resin composites it may be concluded that irreversible changes take place at the fiber/resin interface on thermal treatment which lead to a decay of interface properties. In order to assess the contribution of the matrix material to these changes, test specimens made from the same resin formulation as used in the composite preparation were subjected to the same degradation conditions at 210°C as the composite specimen. Moisture absorption data are summarized in Table XIX and are plotted in Figure 25. It is seen that weight losses occurred on exposure to dry conditions in addition to the loss of initial water (0.43%) identifying the resin matrix as the source for the analogous weight loss observed in the graphite fiber/epoxy resin composites. The initial rate of moisture absorption, as obtained from the tangent, is 9%/day, from which a rate of 2.7%/day may be estimated for a composite of 30 wt. % resin content. This

TABLE XVIII

FLEXURAL STRENGTH AND MODULUS OF THERMALLY TREATED COMPOSITE SAMPLES (PSI)*

			Time Of Exposure (Days)	
	Control		3	10
190°C	112000/40.2x10^6	DRY	110000/36.2x10^6	114000/39.7x10^6
		WET	112000/38.2x10^6	112000/37.2x10^6
210°C	105000/39.7x10^6	DRY	119000/39.6x10^6	114000/36.5x10^6
		WET	115000/37.4x10^6	114000/37.3x10^6

*Average values from 6 specimens; standard deviations were ± 2%; All samples showed combined tensile/compressive failure.

TABLE XIX

WEIGHT CHANGES (IN PERCENT OF CONTROL) OF EPOXY RESIN SAMPLES @ 210°C

		Days of Exposure			
	Control	1	2	3	10
WET		+3.35	+3.80	+3.95	+3.82
WET/DRY*		n.d.	n.d.	-0.80	-1.15
DRY	-0.43	-0.65	-0.75	-0.80	-1.15
TOTAL MOISTURE		4.00	4.55	4.75	4.97

* Wet samples dried for two days in vaccuo at 85°C

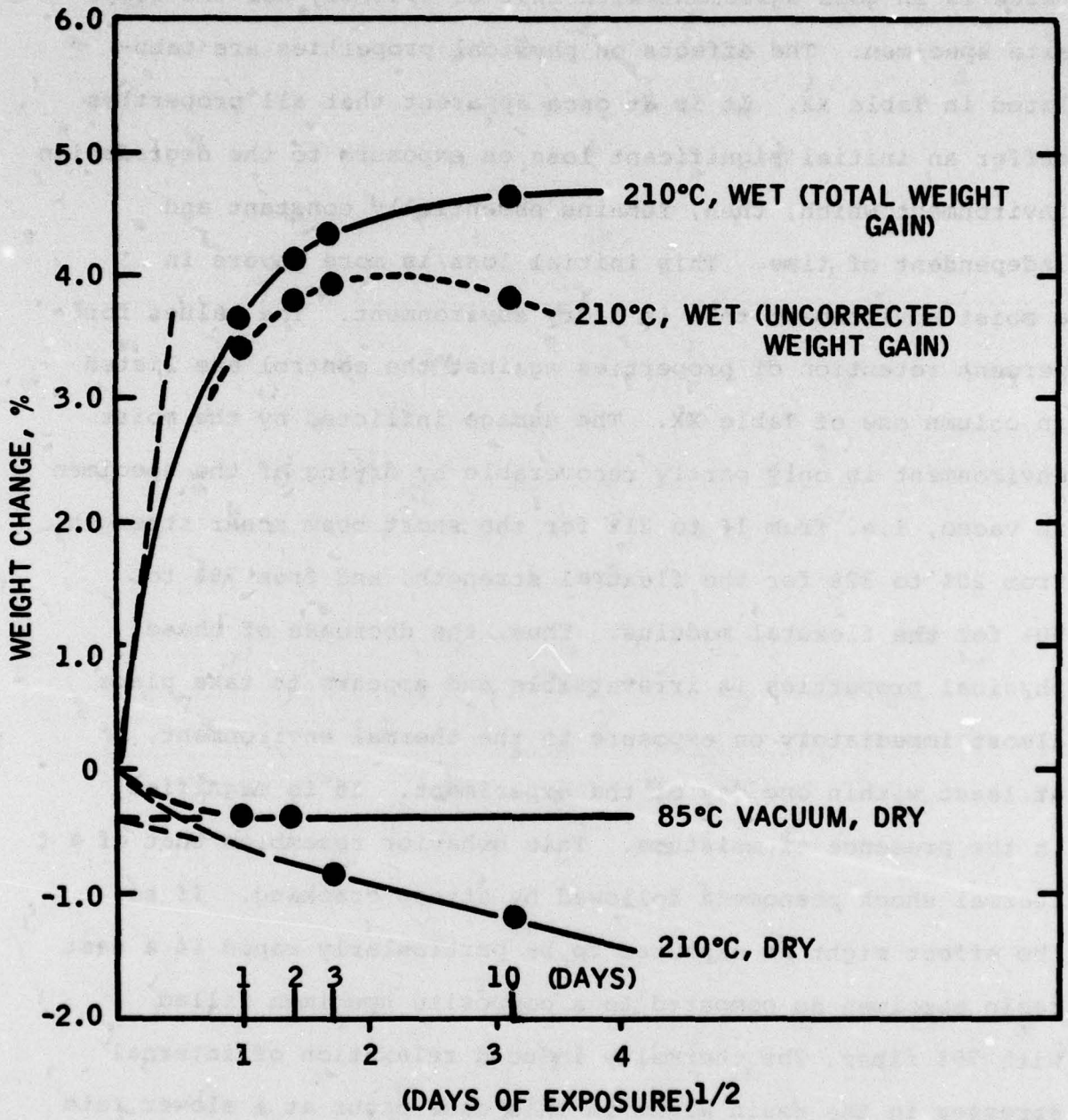

Figure 25. Relative Weight Change of Epoxy Resin Samples on Exposure to Wet and Dry Conditions at 210°C.

value is in good agreement with that of 2.9%/day for the composite specimen. The effects on physical properties are tabulated in Table XX. It is at once apparent that all properties suffer an initial significant loss on exposure to the degradation environment which, then, remains essentially constant and independent of time. This initial loss is more severe in a moist environment than in a dry environment. The values for percent retention of properties against the control are listed in column one of Table XX. The damage inflicted by the moist environment is only partly recoverable by drying of the specimen in vacuo, i.e. from 14 to 21% for the short beam shear strength, from 20% to 32% for the flexural strength, and from 78% to 90% for the flexural modulus. Thus, the decrease of these physical properties is irreversible and appears to take place almost immediately on exposure to the thermal environment, at least within one day of the experiment. It is magnified in the presence of moisture. This behavior resembles that of a thermal shock phenomena followed by stress cracking. If so, the effect might be expected to be particularly rapid in a neat resin specimen as compared to a composite specimen filled with 70% fiber. The thermally induced relaxation of internal stresses in the resin might in this case occur at a slower rate and account for the apparent approach towards a constant decay level as observed in the composite samples (Figure 21).

TABLE XX

PHYSICAL PROPERTIES OF EPOXY RESIN SAMPLES (in PSI) AFTER EXPOSURE TO 210°C*

Condition	Retention Against Control %	Days of Exposure 0	1	2	3	10
SHORT BEAM SHEAR STRENGTH (4:1)						
Wet	14		414±14	448±10	433±44	412±47
Wet/Dry	21				660±80	672±80
Dry	69				2137±94	2242±136
Control	100	3107±99				
FLEXURAL STRENGTH (16:1)						
Wet	20		3170	3760	3100±100	2720±60
Wet/Dry	32				4790±70	4990±200
Dry	85				12750±800	12900±500
Control	100	15000±200(1)				
FLEXURAL MODULUS						
Wet	78		330000	340000	340000	343000
Wet/Dry	90				390000	370000
Dry	100				440000	449000
Control	100	434000(1)				

* Standard deviation given is for n = 6

(1) at 5% strain

8. COMPOSITE DEGRADATION MECHANISM

Considering the total data base collected in our work on the thermal degradation of tagged fiber, fiber/resin composites and neat resin specimen, it appears that the irreversible decay of physical properties in a graphite fiber/epoxy resin composite orginates in the deterioration of the epoxy resin matrix rather than in the deterioration of chemical bonds at the fiber/matrix interface. This conclusion is consistent also with the finding that only 1.5 % of the available fiber surface contains chemical bonds capable of interacting with the resin matrix. In order to rationalize the observed rate of strength decay as a function of interface bond cleavage the assumption would have to be invoked that interface strength is solely composed of the cohesive strength of chemical bonds between fiber and resin, i.e. without contribution of adhesive forces at the interface, and that all the water absorbed into the composite would be concentrated at the interface to provide a 100% R_H environment. Even then, the complication arises that the activation energy of the bond cleavage process is considerably higher (16.3 Kcal/mole) than that of the strength decay process (6.6 Kcal/mole), and that the degradation reaction in the composite takes place in an environment which continuously increases in moisture level. On this basis, the decay rate would be expected to increase with time rather than to decrease as experimentally observed.

Internal stress relaxation of epoxy/resins on exposure to elevated temperatures and moisture has been observed previously, and the formation of micro cracks has been demonstrated (Reference 3). The mechanism of strength loss in graphite fiber/epoxy resin composites at elevated temperatures which was proposed based on this work on neat resins, has been further corroborated by our results which involved a detailed examination of the degradation kinetics of the fiber/resin interface and of the fiber/resin composite. These results indicate that the strength decay exhibited by composites at elevated temperatures, particularly in a moist environment, affects primarily interface properties as measured by interlaminar shear strength and not tensile type strength data which are primarily determined by fiber strength properties. Strength losses of this type may be expected to be reversible by removal of water from the matrix and elimination of the concurrent plasticizing effect on the resin. The same would be predicted from our data for resin dominated composite properties, as flexural strength and modulus, if experiments are carried out at a low temperature regime, e.g. below 100^{o}C. This reversibility of properties at lower temperatures has been frequently reported (Reference 3, 4). By contrast, thermal exposure of the composite to temperatures near or above the glass transition temperature of the matrix resin, which decreases from 180^{o}C rapidly to 120^{o}C at 5% moisture gain, causes a rate discontinuity of the volume change in the resin, but not in the fiber. Stresses created by this effect are known to be relieved via the increased internal mobility of molecules within the resin.

They may lead to an amplified motion of the mobile matrix phase against the immobile fiber phase. This differential motion would act upon the weakest area of the composite, i.e. the interface, leading eventually to localized flaw formation. Failure of the composite structure by application of external forces would take place by stress propagation from these flaws, whereby shear forces would be expected to exert a larger influence on the failure mode than tensile forces. In fact, it might be argued that tensile forces applied to a unidirectional composite might reduce the effect of flaws due to the compressive stresses on the matrix. This effect would minimize the strength losses of a thermally exposed composite at this testing condition. Although the upper use temperature of these type of composites is expected to be 350°F (186°C), degradation experiments were carried out up to 410°F (210°C), the upper curing temperature of the composite. The objective of extending the temperature range was to assess the presence of any discontinuity effects in rate data which might have occured above the Tg region of the dry resin material (180°C). It will be noted that no rate discontinuities were observed, indicating that even accidental temperature spiking above the limiting use temperature would cause no catastrophic change in the mechanism of the strength decay process.

SECTION IV
CONCLUSIONS

The objective of this investigation was to determine the effects of moisture on chemical interactions at the interface of a specific graphite fiber/epoxy resin composite. Studies to evaluate these effects comprised the determination of the number and type of surface sites on a Celion® GY-70 graphite fiber that are capable of reacting with epoxy groups of the resin matrix; the measurement of the rate of degradation of these sites under dry and humid conditions at elevated temperatures; and a comparison of these rates with rates of the irreversible loss of interface properties of graphite fiber/epoxy resin composites. Experimental techniques employed in the work involved the tagging of surface sites on the graphite fiber with a bromine containing epoxy compound (epibromohydrin), the quantification of tagged sites via Induced Electron Emmission Analysis (ESCA) and Neutron Activation Analysis (NAA), the evaluation of the thermal stability of surface sites by vacuum pyrolysis/mass spectrometry (VPy/MS), and the determination of surface area by the BET method, and the measurement of irreversible changes of interface properties via interlaminar shear strength (ILSS), as compared to matrix properties given by flexural strength and flexural modulus.

The results of the work may be summarized as follows:

1. The concentration of epoxidizable surface sites on Celion^{R} GY-70 graphite fiber is 1.85μM/gm covering 1.5 % of the total available fiber surface, as determined by ESCA and NAA measurements on epibromohydrin tagged fiber.

2. Epoxidizable surface sites are composed of a 96/4 molar ratio of carboxyl/phenolic hydroxyl groups. These commence thermal degradation at 320°C with formation of CO, CO_2, and water. In addition, hydrogen bonded water is strongly held in the resin matrix which is lost only on heating to 210°C. This water causes hydrolysis of epoxidized carboxyl surface groups even under dry conditions, and appears to be a property intrinsic to an epoxy resin.

3. Degradation of epoxidized surface sites under dry and wet conditions follows a first order rate in respect to surface sites with an activation energy of 16.3 Kcal/mole. The kinetics and activation energy of degradation correspond to a classical ester hydrolysis in a neutral medium. The rate of degradation at 100% R_H was ten fold that of the rate at 0% R_H, over a temperature range of 100°C to 210°C.

4. Degradation of Celion® GY-70/epoxy resin composites (EpiRez 508/p,p'-diamino diphenylsulfone) under the same conditions as for epibromohydrin tagged fiber caused an irreversible loss of interlaminar shear strength (ILSS). In contrast to the first order degradation rates of tagged surface groups on fibers, the decay rate of ILSS decreased with time of exposure and tended towards a constant ILSS level. The initial rate of ILSS decay showed an activation energy of 6.6 Kcal/mole which was identical to that for the initial rate of moisture absorption into the composite specimen, indicating that ILSS decay was controlled by the moisture diffusion process. Flexural strength and flexural modulus were not affected by the thermal or hydrolytic treatment.

5. Thermal degradation of neat epoxy resin specimen at 210°C in wet and dry environments indicated that moisture absorption into the composite is controlled by the absorption rate of the matrix resin, and that the resin undergoes irreversible losses of short beam shear strength analagous to ILSS loss of the composite.

From the combined experimental evidence generated in this work, it must be concluded that cleavage of fiber/resin interface bonds may be discounted as the source for the irreversible strength losses experienced in graphite fiber/epoxy resin composites. The fact alone that only 1.5% of the available fiber surface is capable of forming cohesive bonds with the resin matrix,

suggests that adhesive forces are the primary parameter for the strength development in composites. This is further corroborated by the much lower activation energy of the physical property decay as compared to that of cohesive bond cleavage. Instead, it appears more likely that irreversible strength losses in a composite are initiated by flaw formation within the resin matrix and at the fiber/resin interface. These flaws may be assumed to be formed by the increased mobility of the matrix phase against the fiber phase, due to plasticization by water and the simultaneously occuring sharp drop of the matrix glass transition temperature. The location of these flaws at the interface is made highly probable since interlaminar shear properties are mostly affected in an irreversible manner, in contrast to matrix resin dominated properties which are mostly recoverable.

A detailed investigation of the failure surface of graphite fiber/epoxy resin composites, after various thermolytic or hydrolytric exposures, would have to be undertaken to experimentally confirm this proposed failure mechanism.

REFERENCES

1. W. Scheck, letter report to NASA/MSFC, November 1970.
2. T. Reinhart, AFOSR Workshop, U. of Del. (1976).
3. C. E. Browning, AFML-TR-76-153,(March 1977).
4. C. E. Browning, ASTM STP 546(1974), 284.
5. P.H. Kaelble, P. J. Dynes, L. W. Crane, and L. Maus, J. Adhesion 7, (1974), 5.
6. L. C. Bennet, and K. E. Hofer, ITT Research Institute Report for Naval Air Systems Command,(1975).
7. E. L. McKague, Jr., J. E. Halkias and J. D. Reynolds J. Comp. Mat. 9 (1975), 2.
8. K. E. Hofer, M. Stander and P. N. Rao, J. Test. and Eval. 3 (1975),423.
9. P. H. Kaelble, P. J. Dynes, E. Cirlin, J. Adhesion 6, (1974), 23.
10. J. W. Herrick, P. E. Gruber and F. T. Mansur, AFML-TR-66-178 Part I, (1966).
11. P. A. Scola and S. C. Brooks, 25th Soc. Plast.Ind. Mtg., (1970).
12. S. Ergun, 9th Conf. Carbon, (1969).
13. S. Chwistrak, ACS 31 (1971), 437.
14. C. S. Brooks and D. A. Scola, J. Col. Int. Sci. 32, (1970), 561.
15. C. S. Brooks, G. S. Golden, D. A. Scola,Carbon 12 (1974), 609.
16. P. L. Walker, Jr., P. J. Hart, F. J. Vastola, Carbon 5 (1967), 363.
17. V. R. Dietz, E. F. McFarland, Proc. 5th Carbon Conf. 2 (1963), 219.
18. L. Bonnetain, J. Chem. Phys. 56, (1959) 266, 486.
19. R. N. Smith, D. A. Young, and R. A. Smith, Trans. Far. Soc. 62 (1966), 2280.

REFERENCES (cont'd)

20. D. W. McKee and V. J. Mimeault Chem. Phys. Carbon, 8 (1973), 151.

21. P. J. Moller and T. Fort, Jr., Col. & Pol. Sci. 253 (1975), 98.

22. J. S. Perkins, D. S. Smith, and D. Rivin 11th Biennial Carbon Conf. (1973), 349.

23. J. S. Mattson and H. B. Mark, Jr., J. Col. Int. Sci. 31, (1969), 131.

24. J. L. Koeniq and F. Tainstra, J. Comp. Mat. 4, (1970),492.

25. C. LeMaistre, Ph. D. Thesis, Renssalear (1969).

26. J. B. onnet, H. Dauksch, J. Escard and C. Winter, C. R. Acad. Sci. Paris 275 (1972), 1219.

27. S. B. Warner,unpublished results.

28. M. Barber, P. Swift, E. L. Evans, and J. M. Thomas Nature 227 (1970), 1131.

29. B. G. Lippens and J. H. DeBoer, J. Catalysis 4,(1965) 649.

30. C. Pierce and B. Ewing, J. Phys. Chem. 68,(1964),2562.

31. C. Pierce, J. Phys. Chem. 72, (1968), 3673.

32. C. K. Ingold, Chem. Soc., (1936), 22.

33. D. E. Stuetz, unpublished results.

*U.S.Government Printing Office: 1978 — 757-080/490